Journal of Environmental Management 236 (2019) 146–162

Contents lists available at ScienceDirect

Journal of Environmental Management

journal homepage: www.elsevier.com/locate/jenvman

Research article

A screening approach to improve water management practices in undeveloped shale plays, with application to the transboundary Eagle Ford Formation in northeast Mexico

Antonio Hernández-Espriú[a,b,*,1], Brad Wolaver[b], Saúl Arciniega-Esparza[c,d], Bridget R. Scanlon[b], Michael H. Young[b], Jean-Philippe Nicot[b], Sergio Macías-Medrano[a], J. Agustín Breña-Naranjo[d]

[a] Hydrogeology Group, Faculty of Engineering, Universidad Nacional Autónoma de México, Mexico City, 04510, Mexico
[b] Bureau of Economic Geology, Jackson School of Geosciences, The University of Texas at Austin, Austin, TX 78758, USA
[c] Programa de Maestría y Doctorado en Ingeniería, Universidad Nacional Autónoma de México, Mexico City, 04510, Mexico
[d] Institute of Engineering, Universidad Nacional Autónoma de México, Mexico City, 04510, Mexico

ARTICLE INFO

Keywords:
Shale plays
Hydraulic fracturing
Eagle Ford
Water stress
Mexico

ABSTRACT

Hydraulic fracturing (HF) operations have transformed the unconventional energy industry, leading to a global increase in hydrocarbon production. Despite this, only the US, China, Canada and Argentina currently dominate production of unconventional resources, with the majority of shale basins globally remaining unprofitable to develop. An important gap in current water-energy nexus research, which this study addresses, is the assessment of potential water use to satisfy HF procedures in emergent plays. This work presents a screening tool for assessing first-order estimates of water impacts in undeveloped shale plays, testing the approach in the transboundary Eagle Ford (EF) play in northeast Mexico. We couple surface water and groundwater stress indicators derived from global hydrological variables to depict a baseline water stress index. Relative water stress is mapped for proposed blocks to be leased by the Mexican government in the future. We simulate four HF scenarios to assess new total water stress indicators for each block, considering shale production schemes using representative well drilling density (well lateral length(s) per unit area) and HF water intensity (HF water volume per unit lateral length) from existing EF development in Texas. Results suggest that the most feasible management scenario would consider the drilling of ~1360 new unconventional wells/yr with projected HF water use of ~57 Mm^3/yr (0.7% of the total water withdrawals). The remaining scenarios will largely affect groundwater resources. Though applied to the EF in Mexico, this screening tool can assess water use constraints in emerging unconventional plays globally.

1. Introduction

Oil and gas horizontal well drilling and hydraulic fracturing (HF) technologies have transformed the energy industry, leading to a global increase in hydrocarbon production. The U.S. Energy Information Administration (U.S. EIA, 2013) reported in 2013 a 10% growth in global resources of shale and tight formation oil and gas (which we define as unconventional energy resources) from the previous 2011 estimate (U.S. EIA, 2011). Technically recoverable unconventional resources increased from 32 billion barrels of oil [bbl] and 6662 trillion cubic feet of gas [Tcf] to 345 bbl oil and 7300 Tcf of gas. According to these sources, current unconventional deposits are located within 137 formations and 95 basins, distributed across 46 countries, representing an important future global energy resource.

Despite this potential, only the US, China, and Canada currently commercially produce unconventional resources (Annevelink et al., 2016). Most shale and tight formation basins in the world remain undeveloped for two main reasons. First, the energy market drives unconventional production. After a sharp increase, oil prices dropped in early 2016 by ~70%, as did production and exploration in several plays (Hulshof et al., 2016; Ikonnikova et al., 2017). Secondly, environment and public health and safety concerns have been raised

* Corresponding author. Visiting Researcher at the Bureau of Economic Geology, Jackson School of Geosciences, The University of Texas at Austin, Austin, TX 78758, USA.
E-mail addresses: antonio.hernandez@beg.utexas.edu, ahespriu@unam.mx (A. Hernández-Espriú).
[1] Current address: Universidad Nacional Autónoma de México, Facultad de Ingeniería, División de Ing. Ciencias de la Tierra, Circuito Interior S/N, Zip Code 04510, México City, México.

https://doi.org/10.1016/j.jenvman.2018.11.123
Received 15 August 2018; Received in revised form 23 November 2018; Accepted 25 November 2018

Table 1
Summary of relevant research in water footprint associated with hydraulic fracturing activities (organized by chronological order).

Study	Period	Location [Unconventional play(s) or basin(s)]	Reported HF water use in m^3/HF well (year); play or formation (F)			Key findings
			Min	Median or Average (A)	Max	
U.S. Plays						
Ikonnikova et al. (2017)	2010–2016	Texas [Eagle Ford]	NS	~34,200[a]	NS	(1) The number of wells projected to be drilled in 2045 is linearly related to oil price, ranging from 20,000 to 97,000 new wells, at $30 to $100/barrel of oil, respectively, (2) considering an oil price of $50/barrel, 40,000 new wells are expected to use a volume of ~1000 Mm^3.
Scanlon et al. (2017)	2005–2015	Texas [Entire Permian Basin][b]	2270 (2005)	18,900	29,310 (2015)	(1) Conventional wells produce ~13 times more water than oil, in comparison to unconventional wells, 3 times, (2) largest HF footprint is associated with unconventional horizontal wells. HF water use in these wells increased by a factor of ~10–16 during 2008–2015, (3) reuse of produced water can reduce water demand for HF.
Walker et al. (2017)	2003–2014	South Platte Basin, Colorado [Niobara][b]	~4000 (2008)	11,000	~31,000 (2014)	(1) Marked differences among median HF water use for horizontal and vertical wells, were found (11,000 and 1000 m^3, respectively, from 2003 to 2014), (2) produced water totaled 9.4 Mm^3, equivalent to 42% of the total water used for HF, (3) HF water use is 0.63% of the basin's water demand for 2014. Goodwin et al. (2014) also reported values in the order of 11,000 m^3/well from 2010 to 2013, excluding water use for extended horizontal wells.
Chen and Carter (2016)	2008–2014	14 states in USA, including: AR, CA, CO, KS, LA, MT, ND, NM, OH, OK, PA, TX, WV, WY	1000	11,259	30,000	(1) HF water use in these states range from 1000–30,000 m^3, (2) the highest volume was consumed by TX (457.42 Mm^3 to fracture 40,521 wells).
Horner et al. (2016)	2008–2012	North Dakota [Bakken]	NS	7296 (2011)[A] 9006 (2012)[A]	NS	(1) HF water use in North Dakota Bakken grew 5-fold from 2008 to 2012, (2) wastewater volumes grew in parallel, (3) HF demand relies on surface water instead of groundwater.
Gallegos et al. (2015)	2000–2014	U.S. national-scale	670[b]	15,275[b,d]–19,425[b,e]	36,620	(1) A comprehensive, national-scale data on HF water use across USA, (2) in 52 out of 57 watersheds with the highest average HF volumes (> 15,000 m^3/well), ~90% of the wells were horizontally drilled.
Kondash and Vengosh (2015)	2005–2014	U.S. national-scale	NS	15,060; Eagle Ford 23,770; Woodford 1510; Niobara	NS	(1) In the US between 2005 and 2014, shale gas extraction used 708 and 232 Mm^3, respectively, (2) from 2012 to 2014, the annual HF water rates were 116 and 66 Mm^3/year for shale gas and unconventional oil production, respectively.
Mitchell et al. (2013)	2008–2012	Upper Ohio River Basin, Pennsylvania [Marcellus]	1500 (2012)[c]	4,400[c] 16,400[b]	17,500 (2011)[b]	(1) Almost all the HF water use in the Marcellus play is withdrawn from surface water, (2) annual streamflow statistics are more suitable to prevent water withdrawals during the driest years, instead monthly analysis, commonly used by regulatory authorities.
Murray (2013)	2000–2011	Oklahoma	NS	11,350[b] 238.5[c]	15,774	(1) HF water use and volume per perforated interval (15.73 m^3/m) were highest for the Woodford Shale horizontal wells, (2) HF volumes account for less than 1% of statewide freshwater use.
Nicot and Scanlon (2012)	2009-mid/2011	Texas [Barnett, Eagle Ford, Haynesville]	NS	14,900; Barnett 16,100; Eagle Ford 21,500; Tx-Haynesville	NS	(1) Water use for shale gas/oil was < 1% of statewide water withdrawals during the period, (2) local impacts vary with water availability and competing demands, (3) projections of net water use during the next 50 years, total ~4350 Mm^3, peaking at 145 Mm^3 in mid-2020.
Plays outside the U.S.						
Yu et al. (2016)	2016	China [Sichuan Basin]	20,000	NS	30,000	During the next decade, HF water use could reach 20–30 Mm^3 in Sichuan Basin, when shale gas exploitation is projected to be most active.

(*continued on next page*)

Table 1 (*continued*)

Yang et al. (2015)	NS	Southwest China [Fuling]	3096	28,800	46,140		(1) HF water use in this play is higher than in the US plays, (2) there is a correlation between water to satisfy HF and length of laterals.
Johnson and Johnson (2012)	2005–2010	British Columbia, Canada [Horn River Basin (HRB), Montney Basin (MB)]	10,000; HRB 800; MB	34,900[A]; Muskwa[F] 19,500[A]; Evie[F] 8,800[A]; Cadomin[F]	70,000; HRB 13,000; MB		The water volume per fracture stage can vary an order of magnitude depending on the completion method used, which in turn is dictated by the basin's geology.

NS: Not specified.
[A]Average.
[F]Geological formation.
HRB: Horn River Basin.
MB: Montney Basin.
HF: Hydraulic fracturing.
AR: Arkansas, CA: California, CO: Colorado, KS: Kansas, LA: Louisiana, MT: Montana, ND: North Dakota, NM: New Mexico, OH: Ohio, OK: Oklahoma, PA: Pennsylvania, TX: Texas, WV: West Virginia, WY: Wyoming.
[a] Estimated in this work based on the authors' results (HF water use of 1.5×10^3 gal/ft per lateral in 2016, or 18.7 m^3/m; average well length of 6000 ft, or ~1828 m, equals to ~34,200 m^3/well).
[b] Unconventional horizontal wells.
[c] Unconventional vertical wells.
[d] Unconventional oil wells.
[e] Unconventional gas wells.

regarding the water and ecological impacts accompanying unconventional energy resource development. These include surface-groundwater withdrawals associated with HF procedures (Mitchell et al., 2013; Reagan et al., 2015), induced seismicity caused by produced water injection (Lee et al., 2016; Rutqvist et al., 2013), localized geohazards (Kim and Lu, 2018), traffic-related (Goodman et al., 2016) and other threats to biota and ecosystems (Brittingham et al., 2014; Souther et al., 2014; Wolaver et al., 2018a), changes in land use (Cox et al., 2017; Wolaver et al., 2018b), landscape fragmentation (Pierre et al., 2017; Willow et al., 2014), air-water quality degradation (Ahmadi and John, 2015; Pinti et al., 2016), and human health risks (Barcelo and Bennett, 2016). As a result, the response of regulatory agencies globally has been varied, with some governments allowing or incentivizing development and others placing a moratorium on the development of unconventional resources (de Melo-Martín et al., 2014).

Managing sourcing, production, and disposal of water is key to successful unconventional resource development. Many efforts have focused on analyzing water demand for HF, illustrated with case studies from active plays, summarized in Table 1. HF water volumes can vary by an order of magnitude (~1000–70,000 m^3/well), depending on well completion method, climate variability, local stratigraphy, or operator practices. The published literature is mostly limited to local or regional reports in the US energy sector; few studies have been completed for unconventional resource plays outside the US (e.g. Rosa et al., 2018), or those not yet in active development.

Thus, an important gap in current research, which this study addresses, is the analysis of potential water use in undeveloped plays. For example, Vandecasteele et al. (2015) assessed potential impacts of water use for HF on regional water resources within the Baltic Basin (Poland), concluding that 0.03–0.86% of total water withdrawals could be attributed to future shale gas exploitation. For the Sichuan Basin (China), estimates of HF water use could reach 20–30 Mm^3/year, when unconventional production is expected to peak (Yu et al., 2016).

A limitation of these interesting examples is that they rely almost entirely on site-specific data reported by local water agencies—which may not necessarily be available to the scientific community—to evaluate water availability associated with shale exploitation scenarios.

Thus, the aim of this paper is to present a methodology for assessing first-order estimates of water impacts in emerging unconventional plays, using widely-available, global-based hydrological data. We illustrate this method in prospective areas of the so-called Burgos and Sabinas basins and the Burro-Picachos Platform (Fig. 1) in northeast Mexico which have significant unconventional oil and gas potential in Upper Jurassic and Cretaceous shale formations (Stevens and Moodhe, 2015). These deposits correlate with the Eagle Ford play—and other source rocks—in Texas (TX-EF), which is one of the largest unconventional resource plays globally (Fig. 1b). For simplicity of nomenclature, we hereafter referred to this footprint as the *Mexican Eagle Ford play* (MX-EF).

Note that, In the United States, hydrologic data are often freely distributed to interest parties; however, in Mexico and other developing countries, surface water and groundwater data are frequently held in centralized government agencies and are typically difficult—if not impossible—to obtain. This paucity of public data in Mexico hinders natural resource management research, such this study, and imposes the use of externally generated global hydrologic datasets, until policies are changed to make datasets more transparent and available.

To the best of the authors' knowledge, only one study has assessed water limitations for HF development in Mexico (Galdeano et al., 2017). This study used an analysis of local water availability values previously developed and published by Mexico's federal water agency, CONAGUA. Galdeano et al. (2017) evaluated volume of shale hydrocarbons which might be recovered as a function of water availability in watersheds and aquifers within the Burgos and Sabinas basins.

As stated in CONAGUA's regulation (NOM-011-CONAGUA-2015 Norm; CONAGUA, 2015), water availability in ungauged hydrological

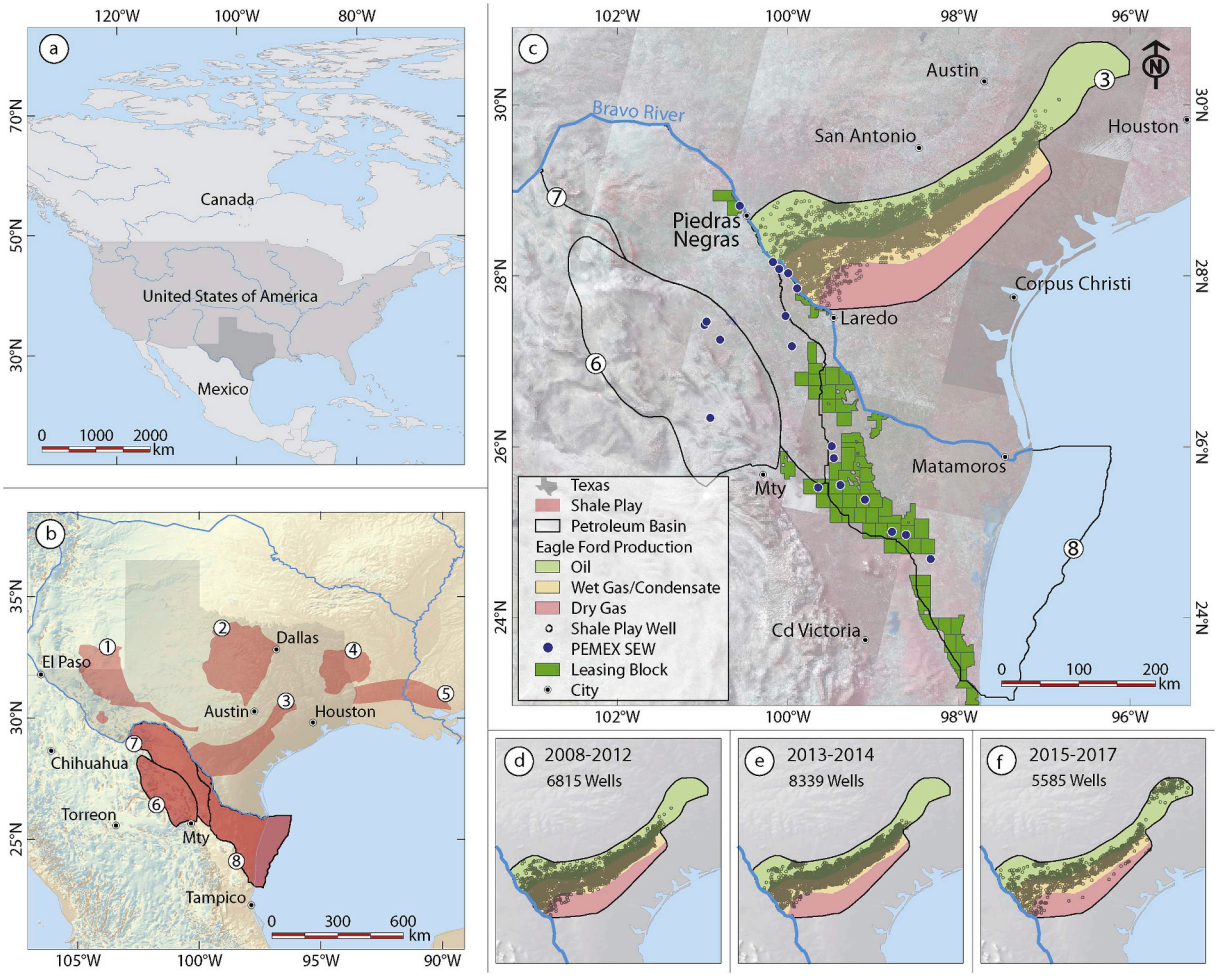

Fig. 1. Geographical setting of the study area: (a) North America, (b) Major Texas Shale plays (1: Permian Basin, 2: Barnett, 3: Eagle Ford, 4: Haynesville, 5: Tuscaloosa in Louisiana) and petroleum basins in Mexico (6: Sabinas, 7: Burro-Picachos Platform, 8: Burgos), (c) Eagle Ford Shale play in Texas, unconventional oil and gas wells in the play (from IHS) and unconventional leasing blocks in Mexico, over a color infrared (vegetation) composite developed by LANDSAT-OLI 8 Imagery from 2017. Unconventional wells drilled in the Eagle Ford play from 2008 to 2012 (from IHS), 2013–2014 (from IHS) and 2015–2017 (from FracFocus) are shown in (d), (e) and (f) respectively. (For interpretation of the references to color in this figure legend, the reader is referred to the Web version of this article.)

basins –a common issue in Mexico– rely on simple rainfall-runoff relationships such as the Rational Formula, RF (Q = precipitation*drainage area*runoff coefficient) and basic assumptions on land cover and soil water storage. The RF approach has several limitations, such as runoff coefficient estimation, because the original values (ASCE-WPCF, 1969) were not created through the calibration of site-specific runoff coefficients in experimental basins, but instead using broad guidelines through consultation with experts, as previously discussed in Grimaldi and Petroselli (2015). Moreover, the RF was originally designed to calculate peak flows in small watersheds and not total runoff (Gupta, 2017).

In our study, we improve upon this approach by providing a broader strategy for analyzing water constraints in prospective and early-stage development shale plays. Our approach combines global-based models of groundwater and surface water availability with local withdrawal rates and illustrated using the MX-EF play (Fig. 1). We depict spatially-distributed groundwater development stress (Alley et al., 2018) in the study area, based on global-scale groundwater parameters (Döll et al., 2014). We also use global mapping of a baseline surface water stress index (Gassert et al., 2015) developed by the World Resources Institute (WRI). We recognize the work of WRI as a valuable tool to estimate water constraints in unconventional plays globally (Reig et al., 2013; WRI, 2014). However, this dataset has numerous gaps in coverage for Mexico (~80%) and globally. In addition, the regional-scale estimates of HF use in the MX-EF by WRI and also Galdeano et al. (2017) are limited because they did not consider oil and gas well drilling density (i.e., well lateral length(s) per unit area) or water intensity (HF volume per unit lateral length), in their estimates of future HF water demands.

Thus, this study builds and improves upon methodological precedents by: (1) developing a screening strategy which relies primarily on global-based hydro(geo)logical data so that water constraints may be assessed for prospective unconventional resource plays globally, (2) investigating for the first time current and future water availability in a transboundary shale play between Mexico and the U.S., (3) reporting updated information about HF water use, drilling density, and water intensity in the TX-EF to inform research on potential water use in the MX-EF (and other plays), and (4) providing a reproducible methodology that can be applied to other emerging plays in the world—particularly in arid/semiarid regions where groundwater will play a key role in ensuring management sustainability to satisfy existing and new highly-demanding users.

2. The transboundary Eagle Ford Shale play

2.1. The Eagle Ford setting in Texas

The Eagle Ford Shale Play of South Texas (TX-EF) is one of the largest oil producers in the U.S. producing ~1 million barrels of oil per

day (EIA, 2017). The play extends across 27 counties, where land is almost exclusively under private ownership (73,146 km^2; Fig. 1b–f; Pierre et al., 2017) and also overlaps with the Eaglebine Shale play, which is a combination of the Woodbine and Eagle Ford Groups (Hentz et al., 2014). The footprint of the study area also includes the Austin Chalk (Martin et al., 2011) and other formations with decades of oil and gas production.

In the TX-EF, almost no horizontal wells were drilled and stimulated prior to 2006, with development expanding rapidly in 2009–2010. Unconventional drilling peaked in 2014 (~3950 wells completed) and dropped precipitously following an oil price decline into 2015 to ~1400 wells in 2016 (Wolaver et al., 2018b). Since then, drilling has been slower in comparison to the Texas development rate, but the play continues to produce ~15% of U.S. oil (RRC, 2018). Currently, the play includes ~17,000 unconventional wells (RRC, 2018).

The TX-EF also straddles important shrub and grassland ecosystems, which have experienced landscape alteration from 95 km^2 in 2008 to 225 km^2 in 2014, as a result of energy development (Pierre et al., 2017). This trend in landscape alteration from well-pad construction is projected to continue for several decades (Wolaver et al., 2018b).

2.2. Water resources

Precipitation ranges from ~560 mm/yr in the semiarid west to ~1100 mm/yr in the more humid east, generating average annual runoff of 5–200 mm/yr (Ryder, 1996). Mean annual evapotranspiration at the Texas-Mexican border ranges from ~410 to 800 mm and mean annual temperature ranges from 19 to 21 °C (Sanford and Selnick, 2013). Several rivers flow across the footprint of the TX-EF, including from west to east, the Rio Grande (known as Rio Bravo in Mexico), Nueces, Frio, San Antonio, Guadalupe, Lavaca and Colorado. Some of rivers receive significant contributions from groundwater discharge through baseflow (Arciniega-esparza et al., 2017; Wolaver et al, 2012).

Along the Lower Rio Grande Valley in Texas, water use (1860 Mm^3/yr) is dominated by irrigation (76%, 1410 Mm^3/yr) and municipal use (21%, 384 Mm^3/yr), followed by livestock and manufacturing (~1% each; TWDB, 2016b; Region M). Note that the volume of water diverted for each category is not necessarily the consumptive use, as some portion of the diversion may flow back to the Rio Grande as a return flow. However, these numbers are valuable as they provide insight into the most important water users.

In South Central Texas, total water demand is ~30% less (1320 Mm^3/yr), reflecting lower irrigation demands (32%, 425 Mm^3/yr), higher municipal (44%, 579 Mm^3/yr), manufacturing (12%, 153 Mm^3/yr) and livestock uses (2%, 30 Mm^3/yr) in addition to cooling water for power generation (6%, 74 Mm^3/yr) and mining (5%, 60 Mm^3/yr), which includes unconventional oil and gas development (TWDB, 2016a; Region L).

Two major groundwater systems overlap and roughly parallel the footprint of the Eagle Ford: (1) the Carrizo-Wilcox aquifer in the northern portion of the play and (2) the Gulf Coast aquifer in the south. The highly productive and regionally extensive Carrizo-Wilcox aquifer is comprised of sand and gravel of Paleocene-Eocene age sediments deposited in a fluvial-deltaic setting, with ~50% of water withdrawals used for irrigation and ~40% for municipal supply (Hamlin and de la Rocha, 2015). The Carrizo-Wilcox aquifer also hosts important brackish groundwater resources (Hamlin and de la Rocha, 2015). The Gulf Coast aquifer system is comprised of three aquifers parallel to the coast and thicken down-dip: The Jasper (Miocene), Evangeline (Pliocene–Miocene) and Chicot (Holocene–Pleistocene) aquifers, which are of fluvial-deltaic origin and consist of laterally discontinuous sand and gravel (George et al., 2011; Kasmarek et al., 2016). See George et al. (2011) for a description of aquifers summarized here.

2.3. Water use and hydraulic fracturing demands

In the TX-EF, historical trends of water use have been progressively increasing over the last 7 years. During 2009 to mid-2011, HF water use per well ranged from 4600 to 33,900 m^3/well with a median of 16,100 m^3/well. Water intensity (HF water use normalized by unit lateral length) ranged from 3.4 to 22.9 m^3/m, with a median of 9.5 m^3/m. (Nicot and Scanlon, 2012).

In 2016, median water use increased to ~33,000 m^3/well, corresponding to a water intensity of 18.7 m^3/m considering median lateral lengths of ~1750 m (Ikonnikova et al., 2017). Overall, water volume to satisfy HF demands totaled 9.1 (2010; 426 wells), 36 (2011; 1558 wells), 47 (2012; 2744 wells) and 67 Mm^3 (2013; 3512 wells) playwide (Scanlon et al., 2014a).

While shale development in Texas historically relied on fresh water sources, brackish groundwater in the TX-EF provides 20% of the total HF water use (U.S. EPA, 2016). The exception is the western portion of the Permian Basin, where brackish groundwater represents 80% of the water footprint to satisfy HF practices (U.S. EPA, 2016).

2.4. Study area within a transboundary context

The Sabinas/Burgos basins (Fig. 1), located across the border from South Texas, have a productive history of conventional hydrocarbon development—and favorable potential for unconventional resources (EIA, 2013). In the Burgos Basin, natural gas production from sandstone reservoirs began in ~1945 with the discovery of the Mision Productor field within the Vicksburg play. Gas production peaked in 2010 and has since declined (PEMEX, 2014). Nevertheless, the Burgos Basin (179 active fields; 2771 conventional wells in 2011) is the major producer of natural gas countrywide, producing 22% and 78% of Mexico's natural gas and nonassociated gas, respectively (Talwani, 2011). On the other hand, The Sabinas Basin tends to be geologically more complex and is mostly within the dry gas window (Stevens and Moodhe, 2015).

Currently, unconventional resources in the Sabinas/Burgos basins remain unexploited, despite its large recoverable potential in the order of 13.1 billion barrels of oil and 545 trillion cubic feet of natural gas (EIA, 2013). Since 2010, the Mexican Petroleum Company (PEMEX) started an exploration assessment which included more than 20 hydraulically fractured wells (located in Fig. 1) targeting correlative shale rocks of the Eagle Ford Formation in south Texas (Stevens and Moodhe, 2015).

For instance, the Emergente-1 well (4701 m depth; 1300 m lateral length) was drilled following a 17-stage frac job using ~30,000 m^3 of water (Stevens and Moodhe, 2015; Zavala-Torres, 2014). After a production test, the Emergente-1 extracted ~2.5 million of cubic feet/day of gas (mcfd) and declined to ~0.3 mcfd in two years (CNH, 2016). At present, none of these wells produced commercial shale resources.

Overall, The Eagle Ford play is a transboundary formation between south Texas and northeast Mexico (Fig. 1). The highly productive U.S. play correlates with the Mexican Jurassic and Cretaceous shale rocks, hosting significant unconventional oil-gas deposits and ranked 6th in terms of shale recoverable resources, worldwide (EIA, 2013). In northeast Mexico, potential limits to Eagle Ford development include truncated structural trends, insufficient burial depth to generate hydrocarbons, or high thermal maturity (Stevens and Moodhe, 2015). Other prospective targets are the Upper Jurassic (Tithonian) Pimienta and La Casita Formations, and formations equivalent to the Agua Nueva Formation of the Tampico-Misantla basin (EIA, 2013).

On March 01, 2018, Mexico's Hydrocarbon Commission (CNH) announced the first unconventional open bid round (Round 3.3). This round comprises nine onshore unconventional blocks in the Burgos Basin, covering an area of 2704 km^2 (www.gob.mx/cnh; last visit: May 2018). A factor which may complicate development of these blocks is uncertainty related to groundwater supplies likely to be used for HF because of limited surface water availability.

The Edwards-Trinity-El Burro is the main aquifer in northeast Mexico. This transboundary aquifer extends across south Texas and northern Mexico (~130,000 km^2; IGRAC, 2015). A lack of formal U.S.-Mexico collaboration and establishment of mutual groundwater development criteria complicates successful management of this important transboundary aquifer (Eckstein, 2011, 2013; Evans, 2006; Duran-Encalada et al., 2016). Within the footprint of the MX-EF play, groundwater resources include (1) a regionally-extensive shallow water-table aquifer comprised of alluvial sand and gravel associated with and in hydraulic connection with the Rio Bravo/Rio Grande river, underlain by (2) an artesian aquifer composed of karstic limestones correlating to the Upper Edwards-Trinity aquifer in Texas. A multi-aquitard group separating both aquifers consists of low permeability deposits, including, from base to top, the regressive sequences of the Eagle Ford (one of the target units), Austin and the Upson shale to shaley-limestone formations (Antuñano, 2001), among others.

With the exception of the Rio Bravo/Rio Grande along the Mexico-U.S. border (Fig. 1b and c) and the Sabinas, San Juan, and Salado Rivers in Mexico, most streams are intermittent. Due to scarce surface water, the region strongly relies on groundwater resources. Fifteen Groundwater Management Units (GMU) overlie the MX-EF play (CONAGUA, 2016). Of these, one third currently experience groundwater overdraft according to official estimates of sustainable aquifer development (CONAGUA, 2016).

Within the MX-EF play, official groundwater abstraction totaled ~530 Mm^3 from ~6600 water wells (2004–2011). Irrigation accounts for ~75% of the groundwater use (~400 Mm^3) followed by industry (12%, 66 Mm^3), municipal (10%, 50 Mm^3), and livestock and other minor uses (3%, 17 Mm^3). However, for management purposes, permitted groundwater production is ~30% higher than actual (e.g. official) pumpage in the order of 680 Mm^3 (CONAGUA, 2016), according to water balance studies as reported by the CONAGUA (available at http://sigagis.conagua.gob.mx/gas1/sections/Disponibilidad_Acuiferos.html, last visit: May 2018). There are uncertainties in relation to these groundwater abstraction figures in the study area and throughout Mexico.

3. Methods and materials

The conceptual framework of this study is divided in three main parts (Fig. 2): (1) evaluation of HF water footprint in the TX-EF play, (2) analysis of current water stress in the MX-EF play, and (3) estimation of water management scenarios necessary to satisfy water demands of potential unconventional resource production in the MX-EF play.

3.1. HF water footprint in the Texas Eagle Ford play for 2015–2017

Recent HF water use and unconventional well densities (number of wells per surface area) associated with HF activities in the Tx-EF were evaluated for January 1, 2015–December 31, 2017. As large-scale development has not yet occurred in the Mexican side of the play, we consider this period—which includes a rich Texas dataset—to be a proxy for what potential HF demands may be in Mexico. We used FracFocus Chemical Disclosure Registry Version 3.0 (https://fracfocus.org/) and IHS Enerdeq (IHS Energy, 2017) database (Fig. 2a).

FracFocus, a public database managed by the Groundwater Protection Council and the Interstate Oil and Gas Commission, provides well-related information including true vertical depth, HF start and end date and total base water volume (i.e., HF water use). However, water sources are not specified. Thus, a limitation of this dataset is that it is not possible to ascertain if HF water was sourced from surface water, freshwater aquifers, brackish groundwater, treated municipal wastewater, or recycled produced water. IHS Enerdeq provides a proprietary database with further information such as production as reported by the Railroad Commission of Texas. These data are applied to individual wells in the IHS database using an internal algorithm and include well orientation (vertical, horizontal, directional), down-hole survey data, lateral displacement, treatment method, fracturing stages, and total fluid volume (i.e., HF water use).

We selected FracFocus as the main source of HF water use, because the dataset is freely available and therefore can be used to create transparent and reproducible research. IHS database (a proprietary product available only to licensees), on the other hand, was used to assess HF water intensity (water use per unit lateral length) and horizontal densities per surface area. As this valuable information is lacking in FracFocus, we integrated the two data sources.

We explored quality control procedures to assess and resolve (whenever possible) spurious data, including detecting inaccurate units, handling missing values, and distinguishing between mild and extreme outliers using the interquartile range method (Barbato et al., 2011). In IHS, we used the "down-hole survey" data to differentiate between pseudo-horizontal and true horizontal lateral sections (i.e., distance-directional offset values that can aid to track the well borehole path in the subsurface). The latter was defined using a threshold of $\leq 2.5^{\circ}$ between a reference horizontal plane and two successive survey points, following the procedure reported by Scanlon et al. (2017). The play was discretized into 5 km^2 grid size to compute the surface area partially covered by lateral lengths at each cell, calculated as follows:

$$area_i = \frac{\bar{s} * \sum_{j=1}^{n} l_{i,j}}{cell\_area} \quad (1)$$

where $area_i$ is the surface percentage covered by lateral lengths within the *i-th* cell, $\bar{s}$ the orthogonal mean separation between laterals, *li,j* the lateral length corresponding to the *j-th* well within the *i-th* cell, and *cell_area* is a fixed surface equals to 25 km^2. We used GIS tools (QGIS Development Team, 2015) to estimate the $\bar{s}$ variable. Finally, the lateral length density was computed as:

$$density_i = \frac{area_i}{\bar{s} * \bar{l}} \quad (2)$$

where $density_i$ is the lateral density per surface area (number of unconventional wells or laterals/km^2) within the *i-th* cell and $\bar{l}$ the mean lateral length, or any other statistical value, as we further discussed in section 3.3. The well density concept applied here was previously described in Gong (2013) and Scanlon et al. (2014a).

A statistical and spatial analysis was carried out using both datasets to quantify significant values, investigate linear correlations to further evaluate spatial trends of water footprints, and calculate well densities and water intensities related to HF procedures. We examined HF water use as a function of production windows across play; that is: (1) oil, (2) wet gas/condensate and (3) dry gas (Fig. 1b and c), according to the initial gas-to-oil ratio for each well, as previously defined and reported by U.S. EIA (2014). We evaluated differences in HF water demands between each productive window using a one-way ANOVA model (confidence interval: 95%, degrees of freedom: 2, probability threshold, $\alpha = 0.001$) and tested for significance by means of the Tukey's HSD test, assuming that HF water use mean is the same for all production zones (null hypothesis).

We used only freely available and open-source tools during the data analysis and geospatial evaluation: (1) RStudio, an integrated development environment for R (R Core Team, 2015), a programming language for statistical computing and visualization, (2) QGIS 3.0 Girona (QGIS Development Team, 2017) a Geographical Information System (GIS) licensed under the GNU General Public License and (3) Python 3.6.5. (Python Core Team, 2015) a cross-platform, object-oriented language for mathematical modeling and data analysis.

3.2. Current water stress analysis in the Mexican Eagle Ford play

Water stress analysis in the MX-EF (Fig. 2b) was assessed by means of coupling surface and groundwater stress indices to compute the Total Water Stress Index, TWSI, for each unconventional leasing block

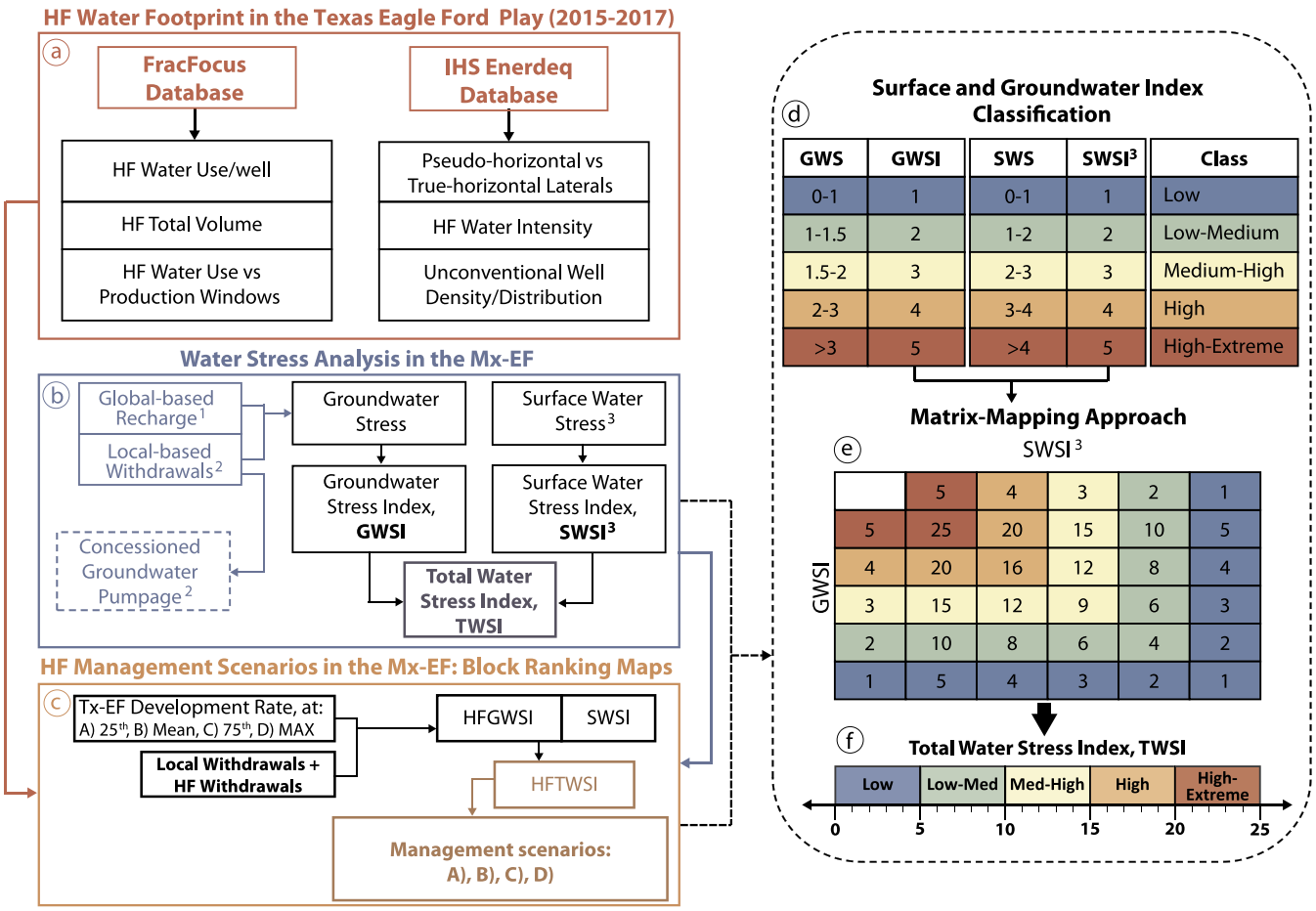

Fig. 2. Conceptual framework showing the proposed methodology employed in this research.

(Fig. 1c) considering all the current uses. The global map of the baseline surface water stress index published by the World Resources Institute (WRI) within the Aqueduct Water Risk Atlas framework (Aqueduct) was used directly as the surface water stress index (SWSI). Aqueduct is a publicly available, global database and interactive tool that maps indicators of water-related risks (http://www.wri.org/resources/data-sets/aqueduct-global-maps-21-data; last visit: May 2018), using geospatial and statistical models to translate global hydrological data into straightforward indicators and aggregated scores (Gassert et al., 2015).

As reported by WRI, SWSI variable measures the ratio of total annual surface water withdrawal relative to the available surface water (Reig et al., 2013), computed as the runoff plus all water flowing into the catchment, where consumptive use is removed in upstream catchments prior to being counted (Gassert et al., 2015). Catchments were extracted by WRI from the Global Drainage Basin Database (Masutomi et al., 2009), while water withdrawals from the Food and Agriculture Organization of the United Nations Aquastat Database (Kohli and Frenken, 2015) and the Pacific Institute World's Water (Gleick, 2014), were acquired by WRI. In addition, raw values were normalized over a set of thresholds, to transform a hydrological variable (*Surface Water Stress*, SWS) into a scored index indicator (*Surface Water Stress Index*, SWSI) based on previous criteria (Vörösmarty et al., 2000).

As a result, five categories or classes of SWSI were established by WRI, from low to high-extreme (Fig. 2d). The SWSI was designed as a long-term index (1950–2010) to reduce the effect of multi-year climate cycles and other short-term complexities, including nonexistent data. See Gassert et al. (2015) and Reig et al. (2013) for details on the data selection, hydrological framework, aggregation and scoring, which are summarized here.

On the other hand, we estimated Groundwater Stress (GWS) as (Alley et al., 2018; Kundzewicz and Döll, 2009):

$$GWS = \frac{Q_{CD}}{R} \quad (3)$$

where Q_{CD} is the total groundwater withdrawals considering current demands and R is aquifer recharge.

We used the global-scale diffuse groundwater recharge map published by Döll et al. (2014) based on the global hydrological and water use model WaterGAP version 2.2a (spatial resolution: 0.5°), which is an improvement on previous versions (Döll et al., 2012; Müller and Schmied et al., 2014). In the cited model, diffuse groundwater recharge (R) from precipitation, global-based soil coverage/type (FAO, 1995; Dirmeyer et al., 2006), and surface bodies were computed; however, the latter is negligible in the study area because of the relative lack of surface water resources in the semi-arid climate of northeast Mexico (CONAGUA, 2016). Thus, R in the MX-EF was considered only as the contribution from rainfall and percolation of irrigation water through soil. The world map of diffuse recharge and model outputs are freely available online (http://www.uni-frankfurt.de/49903932/7_GWdepletion; las visit: June 2018). See Döll et al. (2012, 2014) and Müller and Schmied et al. (2014) for details on the WaterGAP model description, components and outputs are summarized here.

We downloaded monthly values of diffuse recharge from 1960 to 2009 in netCDF format (Network Common Data Form), which are readable files in QGIS and other GIS systems. The monthly values were summed by year and averaged over the 49-year period to minimize effects related to climate variability. Therefore, both surface and groundwater components should be considered as long-term stress

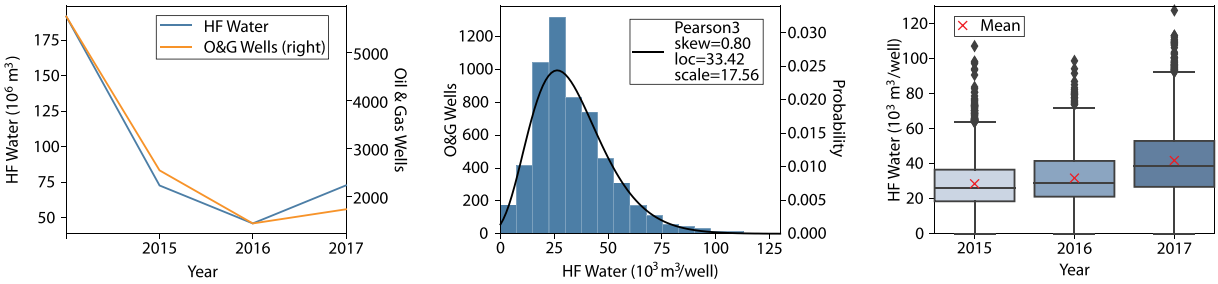

Fig. 3. (a) Total hydraulic fracturing (HF) water use vs unconventional wells for 2015–2017, (b) HF water use histogram and probability density distribution, (c) HF water use/well vs year (source of information: FracFocus).

indicators rather than year-specific values.

To depict GWS (Eq. (3)), site-specific official estimates of groundwater production (maximum allowable abstraction volume per consumptive sector; CONAGUA, 2016) were used as Q_{CD} in the study area. Consumptive sectors include irrigation, municipal supply, industry, and livestock for 2015. These values, assigned by CONAGUA and reported in the Public Registry of Water Rights (REPDA; available online in https://app.conagua.gob.mx/Repda.aspx; last visit: November 2018) are ~28% higher than the actual groundwater pumpage (see Section 2.4). Q_{CD} was expressed as a water depth [L; mm] by summing all the official production rates per well within each leasing block, divided by its surface area.

The GWS raw value was transformed into a five-class scored index indicator (*Groundwater Stress Index*, GWSI) to make it compatible with the surface water component, SWSI (Fig. 2). We fixed the lower threshold between $0 \leq GWS < 1$, which implies that renewable groundwater (R) is larger than the current withdrawals, and thus, groundwater stress is classified as 'low' (GWSI = 1). The remaining classes were estimated by means of the Jenks Natural Breaks algorithm (Jenks, 1977), which is a standard method for dividing a dataset and identifying breakpoints between classes, commonly used in statistical mapping. The five-class indicators are shown in Fig. 2d.

Finally, SWSI and GWSI were coupled by multiplying each row and column (Fig. 2e), resulting in the five-class Total Water Stress Index (*TWSI*) for values from 1 to 25 (Fig. 2f). We used the TWSI as a semi-quantitative parameter to compare baseline water stress within each leasing block in the study area, for further HF projections.

3.3. Water management scenarios to satisfy shale production in the Mexican Eagle Ford play

To simulate the potential effects of shale production in local water resources, Eq. (3) was modified to include additional withdrawals related to HF procedures:

$$HFGWS = \frac{Q_{CD} + Q_{HF}}{R} \quad (4)$$

where *HFGWS* is the modified groundwater stress considering HF and Q_{HF} the potential HF water use. The *HFGWS* parameter was transformed again into a five-class scored index indicator (*HFGSWI*), to make it compatible.

The Q_{HF} parameter was computed by estimating the number of unconventional wells that will potentially be drilled within each leasing block. For this, the results derived in Section 3.1 were used as proxy for future HF demands within the Mexican side of the play. To illustrate water constraints scenarios, the possible number of wells/block in Mexico were determined at a yearly basis as a *fraction* of well density (# laterals/km^2) using representative values from Texas. As such, four management schemes were tested using statistical benchmarks: (A) 25th percentile, (B) mean, (C) 75th percentile, and (D) peak well density in the Tx-EF for 2015–2017. For each case, likely number of wells (A–D) were combined with specific water intensity values (e.g. 25th percentile, mean/median, 75th percentile, max) and results were displayed using a matrix-mapping approach, to support management decision-making in the MX-EF play.

The following assumptions were made: (1) 100% of the water source to satisfy unconventional production will rely on local fresh groundwater, which is more abundant than surface water (CONAGUA, 2016). Thus, a recalculation of the TWSI was conducted (*HFTWSI*) by coupling the *HFGWSI* (Eq. (4)) and the SWSI, which remained unmodified, (2) well density (scenarios A to D) is uniform in all the leasing blocks, and (3) HF water source will come from water wells drilled within the same leasing block, assuming that oil companies will attempt to minimize operational costs. Results of total water stress are presented as ranked maps of lease blocks, for baseline total water stress without HF production (baseline conditions) and for full HF development.

4. Results and discussion

4.1. HF water footprint in the Texas Eagle Ford play for 2015–2017

The volume of water used for HF in the TX-EF play totaled ~192 Mm^3, play-wide based on 5740 unconventional wells (Fig. 3a, source: FracFocus). The number of HF wells and water use varied over time from ~2550 wells with ~73 Mm^3 in 2015, ~1450 wells with ~46 Mm^3 in 2016 and ~1740 wells with ~73 Mm^3 in 2017. Nicot and Scanlon (2012) predicted future water use to satisfy shale production for 2010–2060 based on extrapolations of historical trends in all major Texas plays. They estimated that the TX-EF play will demand a total net water use of 1870 Mm^3 peaking at 58 Mm^3 in 2024. As noted, the peak of this projection was reached and exceeded 11 years earlier (2013; 67 Mm^3; Scanlon et al., 2014a), as well as in subsequent years including 2015 and 2017 with ~70 Mm^3, each year (according to this study).

At a well level, mean, median and interquartile range values were estimated to be 33,424; 29,448 and 21,296–42,708 m^3/well (25th-75th percentiles), respectively. The water footprint frequency histogram per well over the study period (Fig. 3b) can be represented (and reproduced) as a Pearson Type III probability distribution with a location parameter of 33.42×10^3 m^3, scale parameter of 17.56×10^3 m^3, and a skewness of 0.80 (Fig. 3b).

Although during this study period unconventional drilling was highest in 2015 and decreased ~40% in 2016 with a slight recovery in 2017, water use per well has progressively increased: median ~26,300 m^3/well in 2015, 29,000 m^3/well in 2016, and 38,600 m^3/well in 2017. The increasing trend in water use is consistent with previous studies in the TX-EF play (Ikonnikova et al., 2017; Scanlon et al., 2014a). Overall, HF water use/well showed a 2.5-fold increase in just six years, from 2011 (Nicot and Scanlon, 2012) to 2017 (this study).

Moreover, variability in HF water use on a per well basis among the production windows is notable (Fig. 4). In 2015, for instance, water demand in the oil zone was higher (median: ~30,000 m^3/well) than in the dry gas (median: ~25,500 m^3/well) and condensate or wet gas window (median: ~25,000 m^3/well). Similar variances are found in the

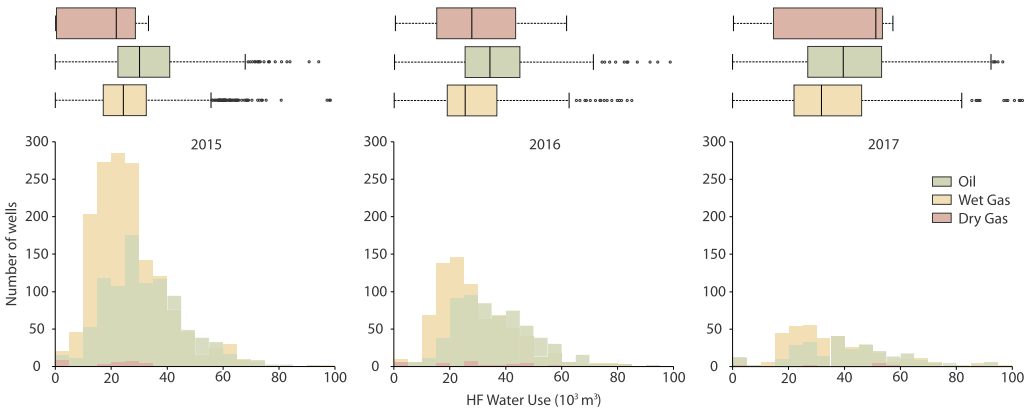

Fig. 4. (a) Histograms showing total hydraulic fracturing (HF) water use as a function of production windows across the Eagle Ford play (oil, wet gas/condensate, dry gas) and (b) boxplots separated by year and production windows, showing HF water use/well for 2015–2017 (source of information: FracFocus).

2016 and 2017 (Fig. 4).

Although spatial variability in HF water use has been noted previously (e.g. Nicot and Scanlon, 2012; Scanlon et al., 2014b), such variability is often overlooked. Thus, we further examined these outcomes by means of statistical tools. The results show that the mean difference, Δμ, between oil-dry gas, wet gas-dry gas and wet gas-oil for 2015–2017 is 8904 ($p < 0.001$), 2601 ($p > 0.001$) and $-6303\ m^3$/well ($p < 0.001$), respectively, suggesting that there is a statistically significant difference in the HF water use between oil and gas zones ($p < \alpha$). In contrast, there is no statistically significant difference between dry and wet gas windows ($p > \alpha$). Therefore, we can assume that mean HF water use in the study period is statistically ~20% higher in unconventional oil wells than in gas wells. Overall, well lateral lengths also vary spatially, decreasing by a 1500–4500 m depth of lateral to the southeast (Fig. 5a), in concordance with the northwesterly structural gain of the play as a result of Laramide-related deformation caused by uplift of the Sierra Madre Oriental in Mexico (Goldhammer, 2001; Hammes et al., 2014). A clearer perspective of this behavior is shown in the three-dimensional view in Fig. 6.

The highest well density over the nine-year production period corresponds to 1.2–3 unconventional wells per km^2 (well laterals/km^2) in hotspots along the central part of the play (Fig. 5b), while over the study period (2015–2017) this value decreased to ≤ 0.6 laterals/km^2 with some isolated spots of 0.6–3 laterals/km^2 over a 5 km^2-grid configuration (Fig. 5c). For comparison, Scanlon et al. (2014a) reported higher well lateral densities from 2009 to 2013, in the order of 0.19–5 well laterals/km^2.

Over the three-year period, median water intensity accounted for ~23.3 m^3/m (Fig. 5d), with an interquartile range of 17.45–25.94, 21.47–28.12 and 20.73–27.91 m^3/m (25^{th}-75th percentiles), for 2015, 2016 and 2017, respectively. Our well density estimates totaled 0.039, 0.138, 0.092, 0.177 and 1.032 well laterals/km^2, considering the 25th, mean, median, 75th and maximum value for 2015, respectively, which represents the density peak within the study period (Table 2).

Overall, water intensity has been steadily increasing over the last years in the Eagle Ford (and other major plays in Texas), from a median value of 9.5 m^3/m in 2009–2011 (Nicot and Scanlon, 2012), to 12.5 m^3/m in 2010–2013 (Scanlon et al., 2014b) or 18.7 m^3/m in 2016 (Ikonnikova et al., 2017). Thus, water intensity, similar to HF water use/well, showed a ~2.3-fold increase in just seven years.

4.2. Current water stress analysis in the Mexican Eagle Ford play

The baseline surface and groundwater stress indices (without examining shale production effects), is depicted in Fig. 7. According to a five-class map indicator, SWSI map shows high to extremely high water stress. Considering a total of 120 unconventional leasing blocks, ~50% of them (56 blocks) were classified as extremely-high class index, followed by low (26%), medium-to-high (7%), low-to-medium and high classes (6%).

In contrast, baseline groundwater is more abundant in the MX-EF play than surface water (Fig. 7b). In this case, ~80% of the leasing blocks (96 blocks) were categorized as a low stress class, followed by an extremely-high zone with 10%, that is, 12 blocks. The other nine blocks are distributed among the remaining classes. Overall, permitted groundwater withdrawal within all blocks totaled ~286 Mm^3.

Although groundwater recharge from precipitation and soil coverage (Döll et al., 2014) is relatively low, i.e., 10–20 mm/yr in the southern part of the Burgos Basin (2–4% recharge coefficient), 5–10 mm/yr in the central blocks between the cities of Monterrey and Piedras Negras (1–2% recharge coefficient) and < 5 mm/yr in the Sabinas Basin (< 1% recharge coefficient) located at the northwestern sector of the study area, ~77% of the groundwater management units show positive availability values according to official figures reported by CONAGUA in 2015 (available at http://sigagis.conagua.gob.mx/gas1/sections/Disponibilidad_Acuiferos.html, last visit: May 2018). Thus, our groundwater stress estimates seem plausible.

The baseline total water stress as a result of coupling both surface and groundwater indices (Fig. 7; right map) shows that ~50% (60 blocks) are in the low zone, ~30% (36 blocks) in the low-to-medium and ~14% (16 blocks) are in the extremely-high zones, suggesting that, eight out of each ten blocks are distributed along the low to medium stress classes, while only ~1.5 blocks are classified in the high to extremely high-water stress zone (Table 3).

4.3. Water management scenarios to satisfy shale production in the Mexican Eagle Ford play

Once the baseline water stress was established (Fig. 7), Eq. (4) was used to simulate potential effects of shale production in the MX-EF play, considering additional withdrawals related to HF. To properly allocate the 'Q_{HF}' term (potential HF withdrawals) we consider the following management scenarios as a function of fixed well densities exhibited in the Tx-EF play, during the peak year (2015; see Table 2):

- Scenario A – 25th percentile of the well density in the Tx-EF play (0.039 laterals/km2/year)
- Scenario B – Mean rate of the well density in the Tx-EF play (0.138 laterals/km^2/year)
- Scenario C – 75th percentile of the well density in the Tx-EF play (0.177 laterals/km^2/year)
- Scenario D – Maximum rate of the well density in the Tx-EF play (1.032 laterals/km^2/year)

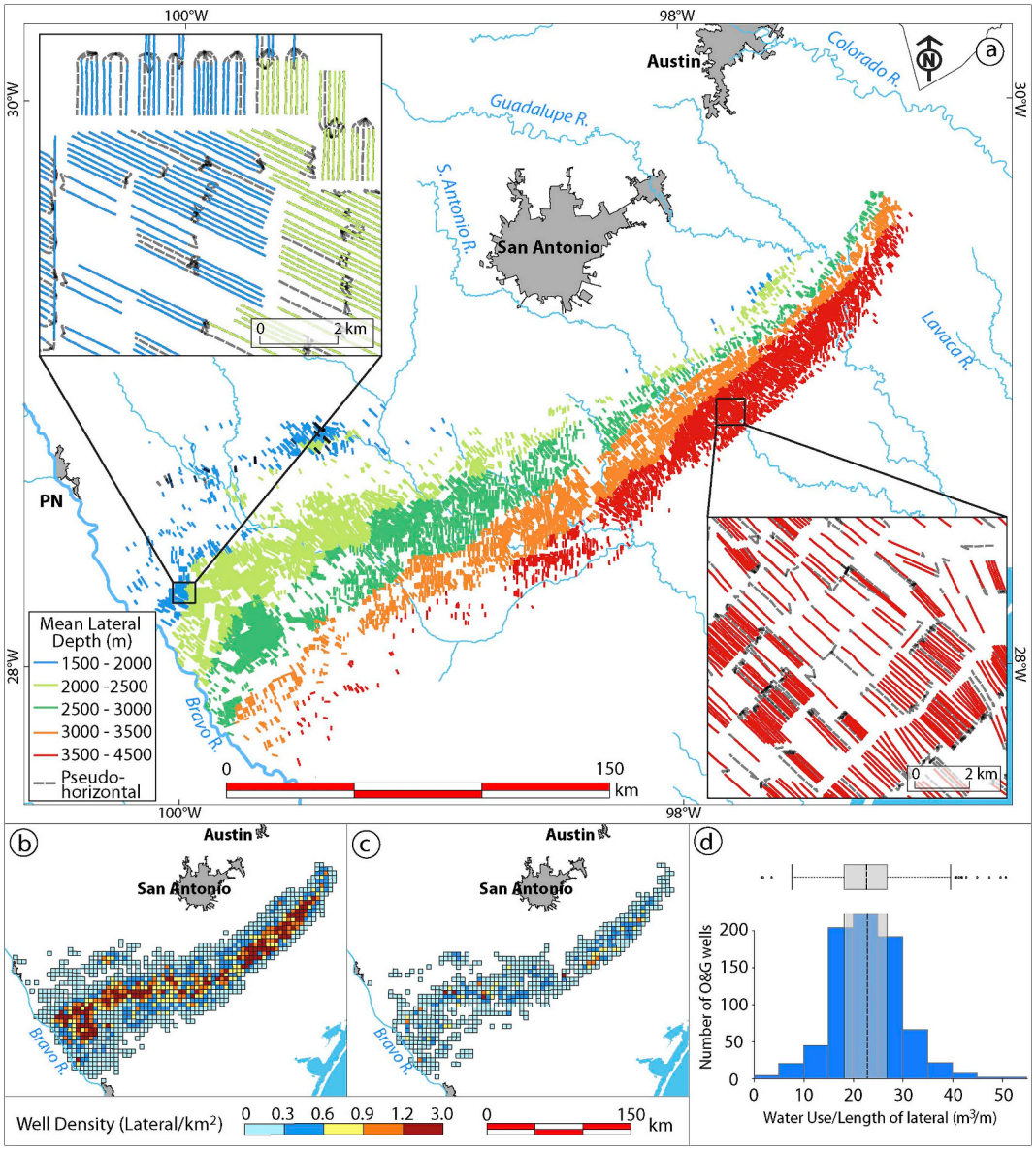

Fig. 5. Spatial distribution of well laterals in the Eagle Ford play for 2009–2017. The insets show a zoomed-in view of the main map. (a), (b) well density in the Eagle Ford play for 2009–2017 and 2015–2017, respectively, expressed as number of well laterals/km^2, (c) hydraulic fracturing water use normalized per unit lateral length for 2015–2017 (source of information: IHS).

In scenario B, we used the mean instead of the median rate, because well density in the former is larger than the latter. Each well density in the TX-EF play was used as a proxy to further compute expected number of oil and gas wells in the MX-EF play region. Within each scenario, we used varying values of lateral lengths and water intensities (Table 2) to depict likely water-energy nexus management schemes in the MX-EF play. Several unconventional block ranking maps categorized by water stress indices were generated as a result, to show relative water availability, block-wide, considering shale production strategies. In this section we present some representative outcomes with additional details in Supplementary Information.

Results show that water stress clearly exceeded both baseline groundwater and total water stress indicators (Fig. 8). Groundwater is much more sensitive to abrupt changes because our main assumption is that HF demand will rely exclusively on shallow groundwater. This is because surface water is scarcer as shown in baseline surface and groundwater stress indices depicted in Fig. 7. In addition, we assume that HF will depend on shallow groundwater (e.g. water table aquifer) as oil and gas companies will try to minimize operational costs during shale development.

Considering scenario B (Fig. 8a, b), the number of leasing blocks within the low TWSI class, decreased from 64 (baseline) to 53, while those in the extremely-high class increased from 16 (baseline) to 23. Overall, blocks within both high and extremely-high classes increased by a factor of two, from 15% (baseline) to ~30%. In this scenario, with a total of 120 blocks covering a surface area of ~35,000 km^2, ~4780 unconventional wells can be drilled, resulting in an HF water demand of ~187 Mm^3/yr. This value represents ~65% of the permitted abstracted groundwater in the study area. Thus, scenario B can largely affect groundwater resources.

Within scenario D, the highest water use scenario, assuming that the maximum well density in the TX-EF play (1.032 well laterals/km^2 for 2015; see Table 2) is uniformly applied in all Mexican leasing blocks, groundwater would be severely impacted (Fig. 8c). A total of 111 blocks out of 120, were estimated to be in the extremely-high class. Moreover, blocks within the high to extremely-high TWSI classes varied from 15% (baseline) to > 70% (Fig. 8d). This analysis clearly demonstrates that the management scenario D is entirely unsustainable from

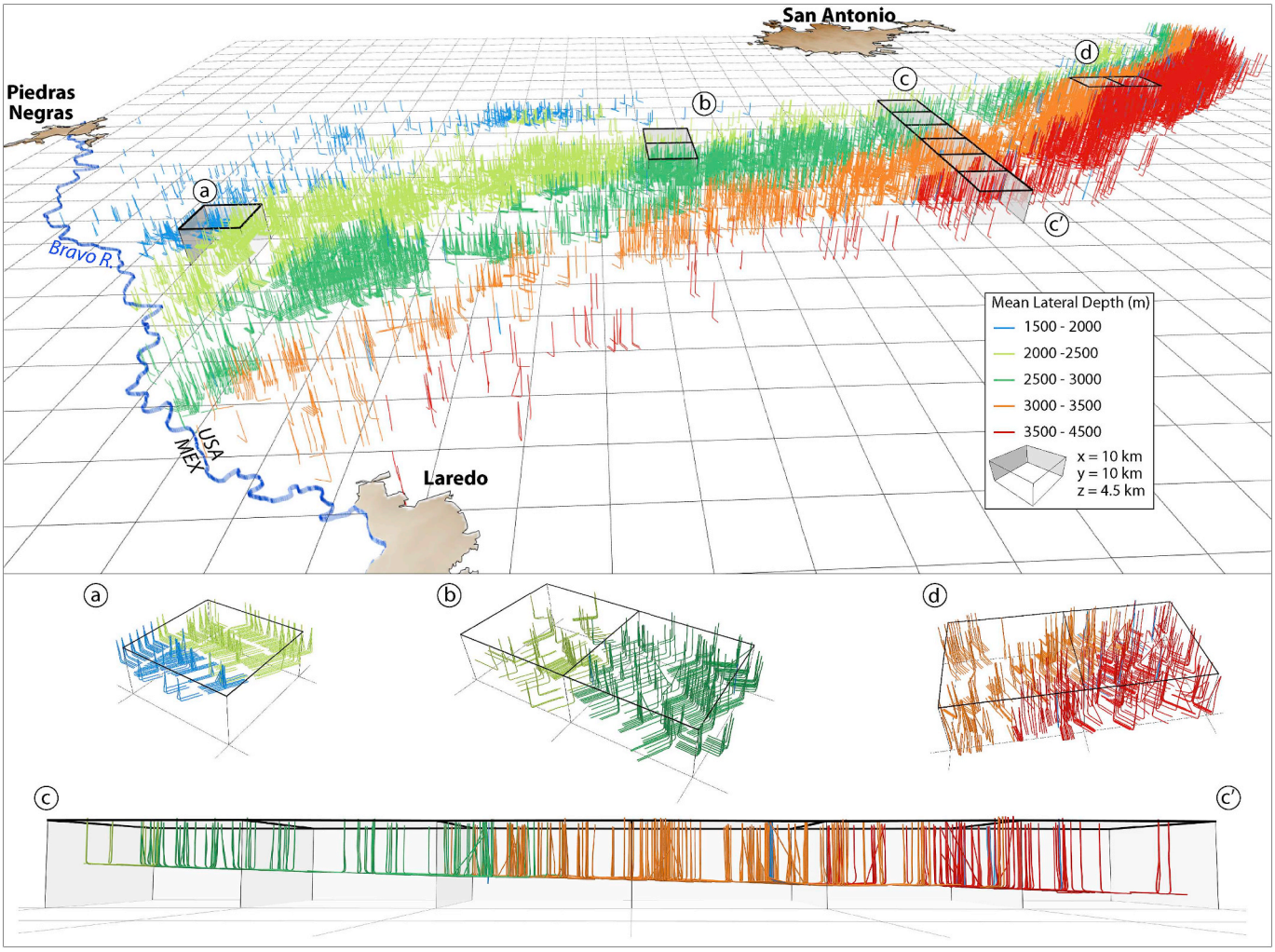

Fig. 6. Three-dimensional view of unconventional wells in the Eagle Ford play for 2009–2017, categorized by its mean lateral depth (source of information: IHS).

an environmental standpoint. This maximum well density would result in drilling ~34,000 new unconventional wells with a projected HF water use of ~1400 Mm^3, which represents a 5-fold increase of the permitted abstracted groundwater volume in the study area. In Section 4.4 we will discuss the limitations of this outcome.

Moreover, sensitivity analysis was conducted, varying lateral length and water intensity within each management scenario, to test the impact of these two variables on water availability at a block level. Take for instance an example given by scenario C. Fig. 9 illustrates the combination of different water intensity and lateral lengths previously computed for the Texas play (Table 2), using in all these cases a fixed well density of 0.177 well laterals/km^2, equals to ~6100 new unconventional wells that can be drilled in the study area.

When simulating the lowest water intensities, that is, a water intensity of 17.54 m^3/m and a lateral length of 1610 m (25th percentile of the TX-EF play), blocks in the low TWSI class decreased from 64 (~50%, baseline) to only 54 blocks (45%), while blocks in the extremely-high class increased from 16 (~13%, baseline) to 21 (~17%). In contrast, the highest values, i.e., water intensity and lateral length of 25.94 m^3/m and 2200 m respectively (75th percentile of the x-EF) can lead to an opposite behavior; that is, blocks within the low and extreme class may vary from 64 to 22 (~18%) and from 21 to 43 (~36%), respectively. We compute HF demands in the order of ~177–359 Mm^3/yr. These HF water net uses fluctuate between ~60 and 100% of the permitted abstracted groundwater volume in the MX-EF play. In the Supplementary Information we present the remaining scenarios (Figs. S2–S4). Projected water use to satisfy HF production is estimated between 57 (scenario A) to 256 Mm^3 (scenario C), representing ~20–100% of the permitted abstracted groundwater volume within all leasing blocks, or in the order of 0.7–3.1% of the total water withdrawals, considering the total water use in Coahuila (2039 Mm^3), Tamaulipas (4215.1 Mm^3) and Nuevo Leon (2069 Mm^3) states for 2015 (CONAGUA, 2016). Table 4 summarizes these findings.

Table 2
Well density, lateral length and water intensity in the Eagle Ford play (Texas) over the study period (2015–2017).

Year	Well Density (# well laterals/km^2/year)					Lateral Length[1] (m)					Water Intensity[a] (m^3/m)				
	25th	Mean	Median	75th	Max	25th	Mean	Median	75th	Max	25th	Mean	Median	75th	Max
2015	0.039	0.138	0.092	0.177	1.032	1613.31	1915.39	1844.65	2229	3575.3	17.54	21.91	21.31	25.94	50.02
2016	0.034	0.117	0.073	0.158	0.945	1615.44	2032.53	1979.98	2483.51	3281.17	21.47	23.8	23.86	28.12	43.31
2017	0.029	0.107	0.069	0.139	1.067	1668.48	2074.37	2029.36	2457.6	3936.19	20.73	24.3	24.71	27.91	47.72

[a] Hydraulic fracturing water use/well, normalized by unit lateral length.[1].

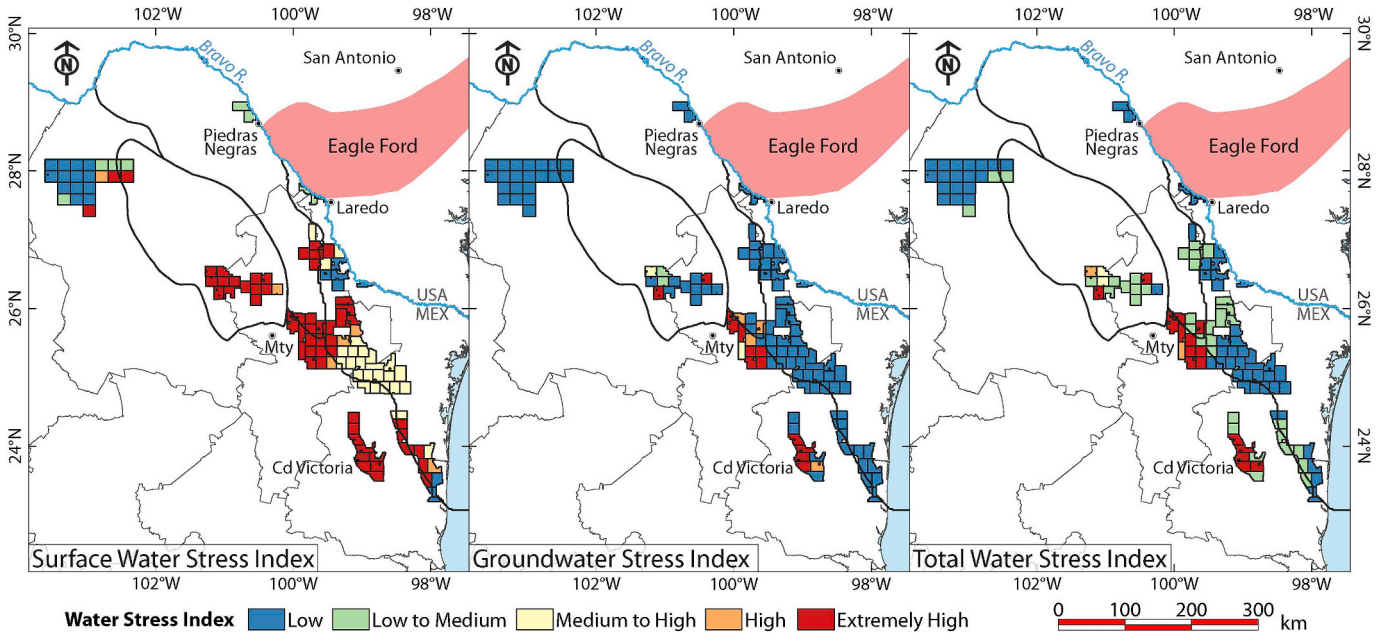

Fig. 7. Baseline surface, groundwater and total water stress, expressed as a five-class index mapping. Squares referred to the unconventional leasing blocks as published by the National Hydrocarbon Commission (CNH), Mexico.

Table 3
Unconventional leasing block counting categorized by baseline surface, groundwater and total water stress index in the Mexican Eagle Ford play.

Class	SWSI		GWSI		TWSI	
	# Blocks[a]	%	# Blocks[a]	%	# Blocks[a]	%
Low	26	21.67	100	83.33	64	53.33
Low to Medium	7	5.83	2	1.67	36	30.00
Medium to High	25	20.83	2	1.67	2	1.67
High	6	5.00	4	3.33	2	1.67
Extremely High	56	46.67	12	10.00	16	13.33

SWSI: Surface water stress index.
GWSI: Groundwater stress index.
TWSI: Total water stress index.
[a] The study area considers a total of 120 leasing blocks.

4.4. Limitations

Several assumptions and limitations have to be considered in this work. As developed, this screening tool relies on shallow fresh groundwater as the sole HF water source. Non-fresh water sources, such as reclaimed, reused, brackish or surface water are not considered in the HF process and even more, recycled water from flowback is considered negligible. However, several active plays inside and outside Texas have been showed that the use of non-fresh water sources (U.S. EPA, 2016; Walker et al., 2017) in combination with recycled water from flowback (Scanlon et al., 2014a) can reduce fresh water stress during HF procedures, avoiding or minimizing competition among water users (e.g. irrigation or domestic supply) and the unconventional industry (Clark et al., 2013; Puls and Sanders, 2017).

Well density in the TX-EF was the main proxy for analyzing potential or expected number of unconventional wells in the Mexican side of the play. This parameter, expressed as the number of wells laterals per surface area (Table 2), was uniformly applied and linearly extrapolated in all the leasing blocks. No spatial nor spatio-temporal variations were simulated during our analysis. This is particularly evident for scenario D.

As shown in Table 4, a maximum well density of > 1 well laterals/km^2 uniformly applied into the MX-EF can lead to an exaggerated number of wells (~36,000 wells in this case). By way of comparison, the highly productive TX-EF play currently exhibits ~20,000 wells over a ten-year production period. Therefore, this scenario clearly overestimates the expected number of wells and thus the projected HF water use, which was computed in the order of ~17% of the total water withdrawals. However, it is a reasonable exercise to examine the full range of possible drilling effects. Excluding scenario D, projected median HF water use is estimated in ~160 Mm^3/yr, which represents between < 1 and 3% of total water withdrawals in the study area. Nicot and Scanlon (2012) reported that water use for shale gas in Texas is < 1% of the statewide water withdrawals, whereas Vandecasteele et al. (2015) estimated that between 0.03 and 0.86% of the total water withdrawals could be attributed to future shale production in northern Poland.

5. Summary and conclusions

This study presents a screening tool for developing first-order estimates of water impacts in undeveloped shale (oil and gas) plays, using prospective areas of the transboundary Eagle Ford play (Sabinas/Burgos basins; Burro-Picachos Platform) of northeast Mexico as a case study. These reservoirs correlate with the footprint of the Eagle Ford play in Texas. An important gap in current water-energy nexus research, which this study addresses, is the assessment of potential water use to satisfy HF in emerging and/or early-stage unconventional plays. In addition, the published literature on water demands of HF is frequently limited to local or regional reports in the U.S. energy sector, thus this study makes an important contribution of extending to Mexico.

This screening method relies mostly (but not only) on global-scale hydrological variables (by coupling surface and groundwater stress indicators) which in general, are more reliable, reproducible, and accessible to the scientific community, than local data produced by local water agencies.

Despite the utility of global studies, on-the-ground data collection and monitoring is critical to improve estimates of groundwater availability and quality—particularly in this semi-arid study area, where surface water sources are limited. We acknowledge that uncertainties in our study could be reduced if access to high-quality local hydrogeologic data were generated and made public available to researchers at no cost, as is the norm for state and federal natural resource management

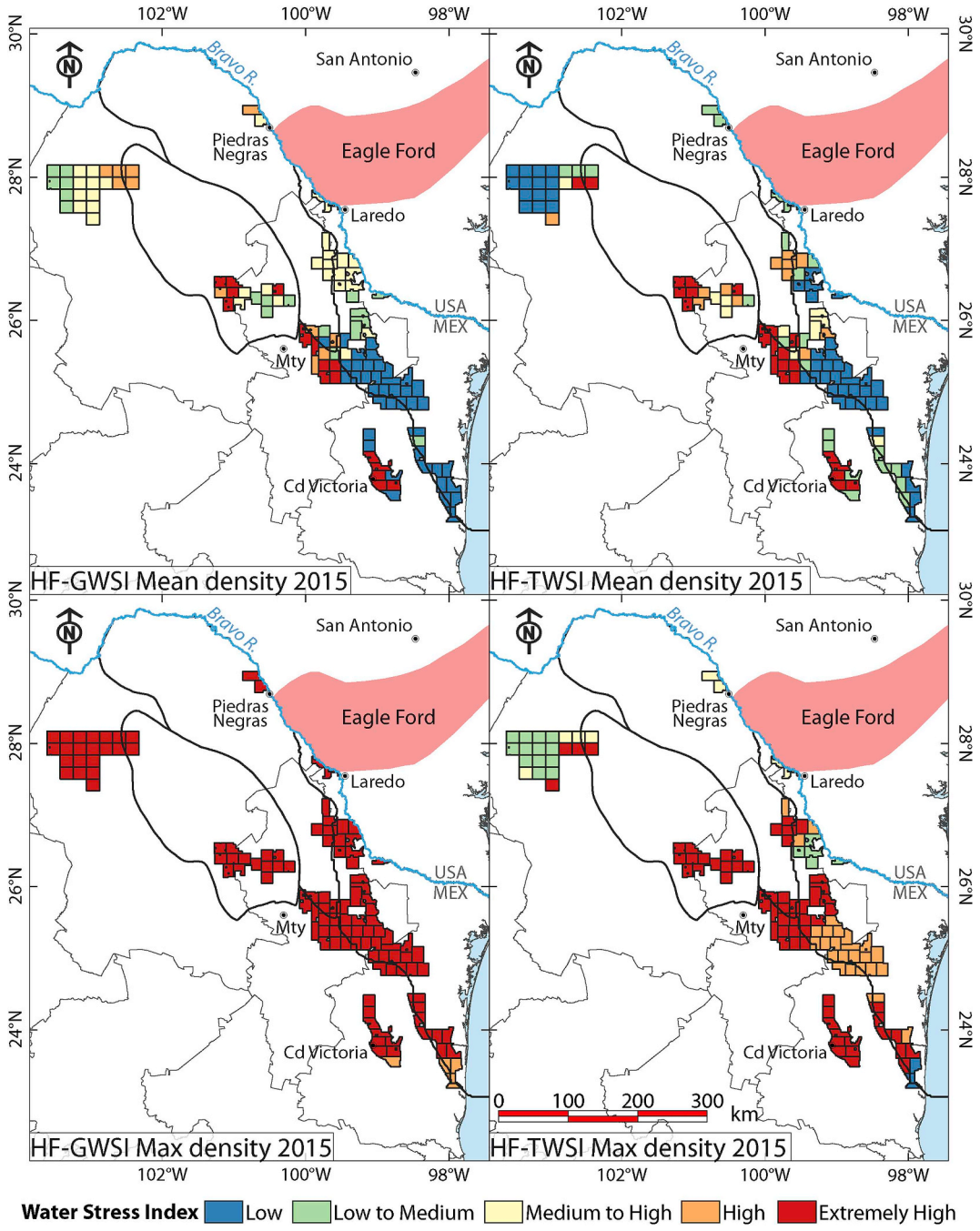

Fig. 8. Leasing block ranking maps showing the spatial distribution of groundwater stress and total water stress index in NE Mexico, due to different hydraulic fracturing development scenarios, based on the mean (above) and maximum (below) well density shown in the Texas Eagle Ford. HF-GWSI: Hydraulic fracturing groundwater stress index; HF-TWSI: Hydraulic fracturing total water stress index.

agencies in the United States.

Our method allowed us to compute baseline surface and groundwater stress indicators to estimate relative total water availability in the MX-EF, across 120 unconventional leasing blocks that the Mexican government will lease over a series of open-bidding rounds in the future. In addition, we simulated HF water use in these blocks using four scenarios (A to D) and a series of sub-scenarios to compute block ranking maps in the study area, categorized by a total water stress index, to assist future management actions.

Across the highly productive Eagle Ford play in Texas, HF water footprints, water intensities, and well densities were estimated in ~21,300–42,700 m^3/well (25^{th}-75th percentiles), ~21–28 m^3 per unit lateral length (25^{th}-75th percentiles) along with median lateral length of ~1900 m, and between 0.039 and 1.032 wells/km^2, respectively, for 2015–2017. Moreover, these variables were used as a proxy to simulate HF water demand for shale production in the MX-EF play. Particularly, well density in the TX-EF was the main proxy for analyzing potential or expected number of unconventional wells in the Mexican side of the play.

Scenario A considers that the MX-EF might be exploited at the 25th percentile rate of the TX-EF, using a well density of 0.039 well laterals/km^2. The remaining scenarios were based on similar assumptions considering a mean rate (scenario B; 0.138 well laterals/km^2), a 75th percentile rate (scenario C; 0.177 well laterals/km^2) and a maximum rate (scenario D; 1.032 well laterals/km^2). With this in mind, scenario A appears to be the most feasible management scheme to produce shale

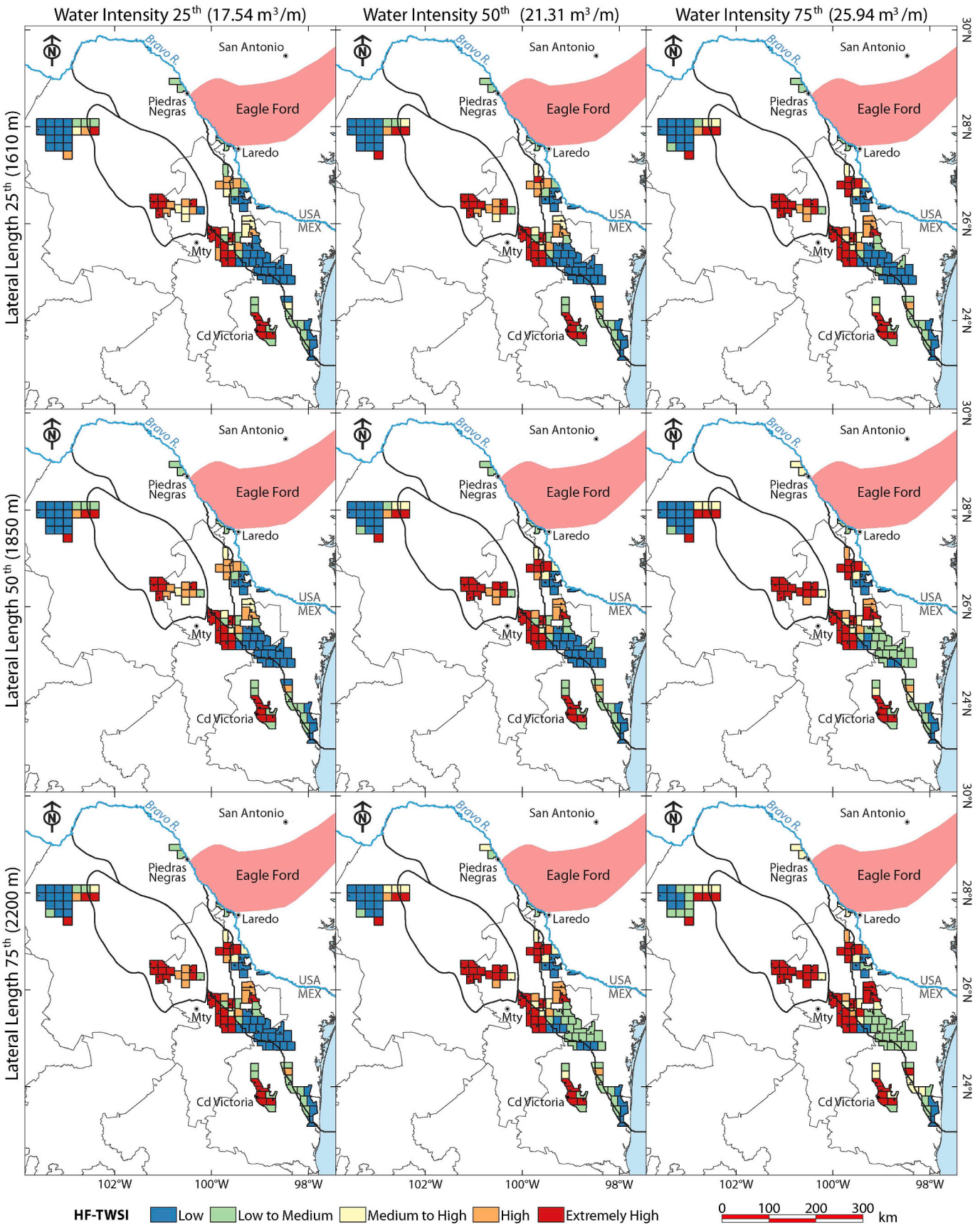

Fig. 9. Matrix-mapping outcome (scenario C) illustrating the combination of different water intensity and lateral lengths previously computed for the Texas play (Table 2), using in all these cases a fixed well density of 0.177 wells/km^2, equals to ~6100 new unconventional wells that can be drilled in the study area.

Table 4
Projected HF water use compared to permitted groundwater volume and total water withdrawals in the study area.

Scenario	Well density (# well laterals/ km^2)[a]	Projected Wells[b]	Area covered by wells per block (%)[c]	HFWU (Mm^3)[d]	HFWU/Permitted groundwater withdrawal [e]	HFWS/Total Withdrawal[f]
A - 25th	0.039	1362	1.22	56.92	19.91	0.68
B - 50th	0.092	3213	2.89	128.06	44.79	1.54
C - Mean	0.138	4819	4.34	195.83	68.49	2.35
D - 75th	0.177	6181	5.57	256.13	89.58	3.08
E - Max	1.032	36040	32.46	1465.66	> 100	17.61

[a] Computed value for the Texas Eagle Ford play in this study (and use it as a proxy for future conditions in Mexico).
[b] Projected number of unconventional wells in the Mexican Eagle Ford play, based on (1).
[c] Area partially covered by unconventional horizontal wells per leasing block (%). We considered that each well lateral will cover an estimated surface area of 1900 m length and 170 m width. Both values are the average lateral length and average separation among two laterals exhibited in the Texas Eagle Ford, for 2015–2017, as computed in this study.
[d] Projected Hydraulic Fracturing Water Use (HFWU) in the Mexican Eagle Ford play.
[e] Hydraulic Fracturing Water Use (HFWU) as percentage of permitted abstracted groundwater use as reported by CONAGUA in the REDPA database.
[f] Hydraulic Fracturing Water Use (HFWU) as percentage of total water withdrawal considering the sum of total water use in the Mexican states of Coahuila (2038.9 Mm^3), Tamaulipas (4215.1 Mm^3) and Nuevo Leon (2068.9 Mm^3) for 2015, as reported by CONAGUA (2016).

gas/oil while protecting shallow groundwater resources. As such, we simulated in this scenario a total drilling of ~1360 unconventional wells/yr with an estimated HF water use of ~57 Mm^3/yr, which represents 0.68% of the total water withdrawals in these prospective leasing blocks. Within scenarios B and C, HF water use would result in a demand of ~196 and 256 Mm^3 (2.4 and ~3.0% of the total water withdrawals, respectively) that will largely affect shallow groundwater. Our main assumption is that 100% of the HF water source will rely on fresh water aquifers that currently supply irrigation, industrial, and domestic sectors.

The main advantage of this screening methodology for assessing unconventional reservoirs, is that a normalized total water availability index can be computed at a leasing block level, with great spatial detail. Overall, to reduce potential water impacts in the study area and in other emergent plays, water authorities should encourage the use of several water sources (reclaimed, reused, surface, groundwater, flowback) and particularly brackish groundwater, to avoid and/or minimize water competition among irrigation and the unconventional industry, to enhanced water-energy management practices in poorly developed plays.

Brackish groundwater, given the scarcity of surface water resources and limited supplies of fresh groundwater in northeast Mexico, will be a critical source for HF operations. Future research directions should include regional-scale brackish groundwater characterization studies, similar to those being conducted in Texas (e.g. Hamlin and de la Rocha, 2015) and elsewhere, to estimate distribution and reserves of non-fresh water supplies. Though applied to the EF in Mexico, this screening tool can assess water use constraints in emerging unconventional plays globally.

Acknowledgments

The first author acknowledges financial support provided by the COMEXUS Fulbright-García Robles Fellowship, the UNAM-DGAPA PASPA and the Matías-Romero (SRE-UT LLILAS) Research Visiting Programs that supported this research. Also, to Scott Tinker and the Bureau of Economic Geology for the hospitality during the sabbatical leave of A. Hernández-Espriú. We are grateful to IHS Enerdeq for granting us access to their database. We truly thank Robert Reedy and Casee Lemons for their technical advices during the databases analysis and also to Rodrigo Oropeza and Fernando Leal for helping out with the statistical work. The authors are grateful for the constructive comments from the Co-Editor-in-Chief J.M. Evans and two anonymous reviewers who have provided valuable feedback that greatly improved the scientific quality of the manuscript. This is the 11th contribution from the Hydrogeology Group (Earth Sciences Division), Faculty of Engineering, UNAM, Mexico.

Appendix A. Supplementary data

Supplementary data to this article can be found online at https://doi.org/10.1016/j.jenvman.2018.11.123.

References

Ahmadi, M., John, K., 2015. Statistical evaluation of the impact of shale gas activities on ozone pollution in North Texas. Sci. Total Environ. 536, 457–467. https://doi.org/https://doi.org/10.1016/j.scitotenv.2015.06.114.
Alley, W.M., Clark, B.R., Ely, D.M., Faunt, C.C., 2018. Groundwater development stress: Global-scale indices compared to regional modeling. Gr. Water 56, 266–275. https://doi.org/10.1111/gwat.12578.
Annevelink, M.P.J.A., Meesters, J.A.J., Hendriks, A.J., 2016. Environmental contamination due to shale gas development. Sci. Total Environ. 550, 431–438. https://doi.org/10.1016/j.scitotenv.2016.01.131.
Antuñano, S.E., 2001. Geologic evolution and gas resources of the Sabinas Basin in northeastern Mexico. AAPG Mem. 75, 241–270.
Arciniega-esparza, S., Breña-naranjo, J.A., Hernández-Espriú, A., Pedrozo-acuña, A., Scanlon, B.R., Philippe, J., Young, M.H., Wolaver, B.D., Alcocer-yamanaka, V.H., 2017. Baseflow recession analysis in a large shale play : Climate variability and anthropogenic alterations mask effects of hydraulic fracturing. 553, 160–171. https://doi.org/10.1016/j.jhydrol.2017.07.059.
ASCE-WPCF, 1969. Design and Construction of Urban Stormwater Management Systems.
Barbato, G., Barini, E.M., Genta, G., Levi, R., 2011. Features and performance of some outlier detection methods. J. Appl. Stat. 38, 2133–2149. https://doi.org/10.1080/02664763.2010.545119.
Barcelo, D., Bennett, J.P., 2016. Human health and environmental risks of unconventional shale gas hydrofracking. Sci. Total Environ. 544, 1139–1140. https://doi.org/https://doi.org/10.1016/j.scitotenv.2015.12.045.
Brittingham, M.C., Maloney, K.O., Farag, A.M., Harper, D.D., Bowen, Z.H., 2014. Ecological Risks of Shale Oil and Gas Development to Wildlife, Aquatic Resources and their Habitats. Environ. Sci. Technol. 48, 11034–11047. https://doi.org/10.1021/es5020482.
Chen, H., Carter, K.E., 2016. Water usage for natural gas production through hydraulic fracturing in the United States from 2008 to 2014. J. Environ. Manag. 170, 152–159. https://doi.org/10.1016/j.jenvman.2016.01.023.
Clark, C.E., Horner, R.M., Harto, C.B., 2013. Life cycle water consumption for shale gas and conventional natural gas. Environ. Sci. Technol. 47, 11829–11836. https://doi.org/10.1021/es4013855.
CONAGUA, 2015. Norma Oficial Mexicana NOM-011-CONAGUA-2015, Conservación del recurso agua, Que establece las especificaciones y el método para determinar la disponibilidad media anual de las aguas nacionales.
CONAGUA, 2016. Estadísticas del Agua en México Edición 2016.
CNH (Comisión Nacional de Hidrocarburos), 2016. Seguimiento a la exploración y extracción de aceite y gas en lutitas, August, 2016. (Open Document).
Cox, A.B., Taylor, N.T., Rebein, M.A., Song, M., Moran, M.D., McClung, M.R., 2017. Land use changes from unconventional gas development in public lands of the fayetteville shale. Nat. Area J. 37. https://doi.org/10.3375/043.037.0212.
de Melo-Martín, I., Hays, J., Finkel, M.L., 2014. The role of ethics in shale gas policies. Sci. Total Environ. 470–471, 1114–1119. https://doi.org/10.1016/j.scitotenv.2013.10.088.
Dirmeyer, P.A., Gao, X., Zhao, M., Guo, Z., Oki, T., Hanasaki, N., 2006. GSWP-2: Multimodel analysis and implications for our perception of the land surface. Bull. Am. Meteorol. Soc. 87 (10), 1381–1398.
Döll, P., Hoffmann-Dobrev, H., Portmann, F.T., Siebert, S., Eicker, A., Rodell, M., Strassberg, G., Scanlon, B.R., 2012. Impact of water withdrawals from groundwater and surface water on continental water storage variations. J. Geodyn. https://doi.org/10.1016/j.jog.2011.05.001.

Döll, P., Müller Schmied, H., Schuh, C., Portmann, F., Eicker, A., 2014. Global-scale assessment of groundwater depletion and related groundwater abstractions: Combining hydrologicalmodeling with information from well observations and GRACE satellites. Water Resour. Res. 6, 446. https://doi.org/10.1016/0022-1694(68)90080-2.
Duran-Encalada, J.A., Paucar-Caceres, A., Bandala, E.R., Wright, G.H., 2016. The impact of global climate change on water quantity and quality: A system dynamics approach to the US–Mexican transborder region. Eur. J. Oper. Res. 256, 567–581.
Eckstein, G.E., 2011. Managing buried treasure across frontiers: the International Law of Transboundary Aquifers. Water Int. 36, 154–161.
Eckstein, G.E., 2013. Rethinking Transboundary Ground Water Resources Management: A Local Approach along the Mexico-U.S. Border. Georg. Int. Environ. Law Rev. 25, 95–128.
EIA, 2017. Annual Energy Outlook 2017 with projections to 2050. J. Phys. A Math. Theor. 3–125 DOE/EIA-0383(2017).
Evans, J., 2006. Transboundary Groundwater in New Mexico, Texas, and Mexico: State and Local Legal Remedies to a Challenge Between Cities, States, and Nations. Wm. Mary Envtl. L. Pol'y Rev. 471.
FAO (Food and Agriculture Organization of the United Nations), 1995. Digital Soil Map of the World and Derived Soil Properties, CD- ROM. Online version in:. http://www.fao.org/soils-portal/soil-survey/soil-maps-and-databases/faounesco-soil-map-of-the-world/en, 3.5 (last visit: Nov., 2018).
Galdeano, C., Cook, M.A., Webber, M.E., 2017. Multilayer geospatial analysis of water availability for shale resources development in Mexico. Environ. Res. Lett. 12.
Gallegos, T.J., Varela, B.A., Haines, S.S., Engle, M.A., 2015. Hydraulic fracturing water use variability in the United States and potential environmental implications. Water Resour. Res. 51, 5839–5845. https://doi.org/10.1002/2015WR017278.
Gassert, F., Landis, M., Luck, M., Reig, P., Shiao, T., 2015. Aqueduct Global Maps 2.1: Constructing decision-relevant global water risk indicators. World Resour. Inst. 31.
George, P.G., Mace, R.E., R. P, 2011. Aquifers of Texas. Report 380. Austin, TX (2011). .
Gleick, P.H., 2014. The world's water, The World's Water. https://doi.org/10.5822/978-1-61091-483-3.
Goldhammer, R.K., 2001. AAPG Memoir 75, Chapter 3: Middle Jurassic-Upper Cretaceous Paleogeographic Evolution and Sequence-stratigraphic Framework of the Northwest Gulf of Mexico Rim.
Gong, X., 2013. Assessment of the Eagle Ford Shale Oil and Gas Resources. PhD Thesis. Texas A&M University, Texas, USA.
Goodman, P.S., Galatioto, F., Thorpe, N., Namdeo, A.K., Davies, R.J., Bird, R.N., 2016. Investigating the traffic-related environmental impacts of hydraulic-fracturing (fracking) operations. Environ. Int. 89–90, 248–260. https://doi.org/10.1016/j.envint.2016.02.002.
Goodwin, S., Carlson, K., Knox, K., Douglas, C., Rein, L., 2014. Water intensity assessment of shale gas resources in the Wat- tenberg field in North eastern Colorado. Environ. Sci. Technol 48 (10), 5991–5995. https://doi.org/10.1021/es404675h.
Grimaldi, S., Petroselli, A., 2015. Do we still need the Rational Formula? An alternative empirical procedure for peak discharge estimation in small and ungauged basins. Hydrol. Sci. J. 60, 67–77. https://doi.org/10.1080/02626667.2014.880546.
Gupta, R.S., 2017. Hydrology and Hydraulic Systems, fourth ed. Waveland Press, Long Grove, IL, pp. 888.
Hamlin, H.S., de la Rocha, L., 2015. Using electric logs to estimate groundwater salinity and map brackish groundwater resources in the Carrizo-Wilcox aquifer in South Texas. Gulf Coast Assoc. Geol. Soc. J. 4, 109–131.
Hammes, U., Eastwood, R., McDaid, G., Vankov, E., Shultz, J., Smye, K., Potter, E., Ikonnikova, S., Tinker, S., 2014. Regional assessment of the Eagle Ford Group of south Texas, USA: insights from lithology, pore volume, water saturation, organic richness and productivity correlations. Igarss 4, 1–5. 2014. https://doi.org/10.1007/s13398-014-0173-7.2.
Hentz, T.F., Ambrose, W.A., Smith, D.C., 2014. Eaglebine play of the southwestern East Texas basin Stratigraphic and depositional framework of the Upper Cretaceous (Cenomanian-Turonian) Woodbine and Eagle Ford Groups. Am. Assoc. Petrol. Geol. Bull. https://doi.org/10.1306/07071413232.
Horner, R.M., Harto, C.B., Jackson, R.B., Lowry, E.R., Brandt, A.R., Yeskoo, T.W., Murphy, D.J., Clark, C.E., 2016. Water use and management in the Bakken shale oil play in North Dakota. Environ. Sci. Technol. 50, 3275–3282. https://doi.org/10.1021/acs.est.5b04079.
Hulshof, D., van der Maat, J.P., Mulder, M., 2016. Market fundamentals, competition and natural-gas prices. Energy Policy 94, 480–491. https://doi.org/10.1016/j.enpol.2015.12.016.
IGRAC, 2015. Transboundary Aquifers of the World Map 2015 [map]. 2015. Scale 1 : 50 000 000.
IHS Markit database [WWW Document], n.d. URL https://www.ihs.com/products/oil-gas-tools-enerdeq-browser.html.
Ikonnikova, S., Male, F., Scanlon, B.R., Reedy, R.C., McDaid, G., 2017. Projecting the Water Footprint Associated with Shale Resource Production: Eagle Ford Shale Case Study. Environ. Sci. Technol acs.est.7b03150. https://doi.org/10.1021/acs.est.7b03150.
Jenks, G.F., 1977. Optimal data classification for choropleth maps. Geogr. Dep. Occas. Pap. 22.
Johnson, E.G., Johnson, L.A., 2012. Hydraulic Fracture Water Usage in Northeast British Columbia: Locations, Volumes, And Trends, Geoscience Reports. Victoria, BN, Canada.
Kasmarek, M.C., Ramage, J.K., Johnson, M.R., 2016. Water-level altitudes 2016 and water-level changes in the Chicot, Evangeline, and Jasper aquifers and compaction 1973–2015 in the Chicot and Evangeline aquifers. Houston-Galveston region, Texas.
Kim, J.-W., Lu, Z., 2018. Association between localized geohazards in West Texas and human activities, recognized by Sentinel-1A/B satellite radar imagery. Sci. Rep. 8, 4727. https://doi.org/10.1038/s41598-018-23143-6.
Kohli, A., Frenken, K., 2015. Renewable Water Resources Assessment – 2015 AQUASTAT Methodology Review, vol. 8.
Kondash, A., Vengosh, A., 2015. Water footprint of hydraulic fracturing. Environ. Sci. Technol. Lett. 2, 276–280. https://doi.org/10.1021/acs.estlett.5b00211.
Kundzewicz, Z.W., Döll, P., 2009. Will groundwater ease freshwater stress under climate change? Hydrol. Sci. J. https://doi.org/10.1623/hysj.54.4.665.
Lee, J.Y., Weingarten, M., Ge, S., 2016. Induced seismicity: the potential hazard from shale gas development and CO2 geologic storage. Geosci. J. 20, 137–148. https://doi.org/10.1007/s12303-015-0030-5.
Martin, R., Baihly, J., Malpani, R., 2011. Understanding production from eagle Ford-Austin chalk system. SPE Annu. Technol. 1–28. https://doi.org/10.2118/145117-MS.
Masutomi, Y., Inui, Y., Takahashi, K., Matsuoka, Y., 2009. Development of highly accurate global polygonal drainage basin data. Hydrol. Process. 2274, 572–584. https://doi.org/10.1002/hyp.7186.
Mitchell, A.L., Small, M., Casman, E. a, 2013. Surface water withdrawals for Marcellus Shale gas development: performance of alternative regulatory approaches in the Upper Ohio River Basin. Environ. Sci. Technol. 47, 12669–12678. https://doi.org/10.1021/es403537z.
Murray, K.E., 2013. State-scale perspective on water use and production associated with oil and gas operations, Oklahoma, U.S. Environ. Sci. Technol. 47, 4918–4925.
Nicot, J.P., Scanlon, B.R., 2012. Water use for shale gas production in Texas, U.S. U.S. Environ. Sci. Technol. 46, 3580–3586. https://doi.org/10.1021/es204602t.
PEMEX, 2014. Presente y Futuro del Proyecto Burgos. Internal Report., 38 p.
Pierre, J.P., Young, M.H., Wolaver, B.D., Andrews, J.R., Breton, C.L., 2017. Time Series Analysis of Energy Production and Associated Landscape Fragmentation in the Eagle Ford Shale Play. Environ. Manag. https://doi.org/10.1007/s00267-017-0925-1.
Pinti, D.L., Gelinas, Y., Moritz, A.M., Larocque, M., Sano, Y., 2016. Anthropogenic and natural methane emissions from a shale gas exploration area of Quebec, Canada. Sci. Total Environ. 566–567, 1329–1338. https://doi.org/https://doi.org/10.1016/j.scitotenv.2016.05.193.
Puls, R., Sanders, L.D., 2017. In: Ziolkowska, J.R., Peterson, J.M.B.T.-C., W.R. (Eds.), Chapter 2.2.3 - Water–Energy Nexus and Environmental Aspects of Oil and Gas Production. Elsevier, pp. 160–177. https://doi.org/https://doi.org/10.1016/B978-0-12-803237-4.00009-4.
Python Core Team, 2015. Python: A dynamic, open source programming language. Python Software Foundation.
QGIS Development Team, 2015. QGIS Geographic Information System. Open Source Geospatial Found. Proj.
R Core team, 2015. R: A Language and Environment for Statistical Computing. R Found. Stat. Comput., Vienna, Austria3-900051-07-0. http://www.R-project.org/.
Reagan, M.T., Moridis, G.J., Keen, N.D., Johnson, J.N., 2015. Numerical simulation of the environmental impact of hydraulic fracturing of tight/shale gas reservoirs on near-surface groundwater: Background, base cases, shallow reservoirs, short-term gas, and water transport. Water Resour. Res. 51, 2543–2573. https://doi.org/10.1002/2014WR016086.
Reig, P., Shiao, T., Gassert, F., 2013. Aqueduct Water Risk Framework. Washington, DC.
Rosa, L., Rulli, M.C., Davis, K.F., D'Odorico, P., 2018. The water-energy nexus of hydraulic fracturing: a global hydrologic analysis for shale oil and gas extraction. Earth's Futur 6, 745–756. https://doi.org/10.1002/2018EF000809.
RRC, 2018. Production Data. [WWW Document]. http://www.rrc.state.tx.us/oil-gas/research-and-statistics/production-data/.
Rutqvist, J., Rinaldi, A.P., Cappa, F., Moridis, G.J., 2013. Modeling of fault reactivation and induced seismicity during hydraulic fracturing of shale-gas reservoirs. J. Petrol. Sci. Eng. 107, 31–44. https://doi.org/10.1016/j.petrol.2013.04.023.
Ryder, P., 1996. Ground Water Atlas of the United States: Segment 4. Oklahoma and Texas, Reston, Virginia.
Sanford, W.E., Selnick, D.L., 2013. Estimation of evapotranspiration across the conterminous united states using a regression with climate and land-cover data1. JAWRA J. Am. Water Resour. Assoc. https://doi.org/10.1111/jawr.12010.
Scanlon, B.R., Reedy, R.C., Philippe Nicot, J.P., 2014a. Will water scarcity in semiarid regions limit hydraulic fracturing of shale plays? Environ. Res. Lett. 9, 124011. https://doi.org/10.1088/1748-9326/9/12/124011.
Scanlon, B., Reedy, R., Nicot, J.P., 2014b. Comparison of Water Use for Hydraulic Fracturing for Unconventional Oil and Gas versus Conventional Oil. Environ. Sci. Technol. 48, 12386–12393.
Scanlon, B.R., Reedy, R.C., Male, F., Walsh, M., 2017. Water Issues Related to Transitioning from Conventional to Unconventional Oil Production in the Permian Basin. Environ. Sci. Technol acs.est.7b02185. https://doi.org/10.1021/acs.est.7b02185.
Schmied, H.M., Eisner, S., Franz, D., Wattenbach, M., Portmann, F.T., Flörke, M., Döll, P., 2014. Sensitivity of simulated global-scale freshwater fluxes and storages to input data, hydrological model structure, human water use and calibration. Hydrol. Earth Syst. Sci. https://doi.org/10.5194/hess-18-3511-2014.
Souther, S., Tingley, M.W., Popescu, V.D., Hayman, D.T.S., Ryan, M.E., Graves, T.A., Hartl, B., Terrell, K., 2014. Biotic impacts of energy development from shale: Research priorities and knowledge gaps. Front. Ecol. Environ. 12, 330–338. https://doi.org/10.1890/130324.
Stevens, S.H., Moodhe, K.D., 2015. Evaluation of Mexico's shale oil and gas potential. SPE 1–13 177139.
Talwani, M., 2011. Oil and Gas in Mexico: Geology, Production Rates and Reserves, James A. Baker III. Institute for Public Policy, Rice University, pp. 34.
TWDB, 2016a. Region L. South Central Texas Regional Water Plan.
TWDB, 2016b. Region M. Rio Grande Regional Water Plan.
U.S. Energy Information Administration, 2011. Annual Energy Review 2011.
U.S. Energy Information Administration, 2013. Technically Recoverable Shale Oil and Shale Gas Resources: An Assessment of 137 Shale Formations in 41 Countries Outside

the United States. U.S. EIA. https://doi.org/www.eia.gov/analysis/studies/worldshalegas/.
U.S. Energy Information Administration, 2014. Updates to the EIA Eagle Ford Play Maps, United States Energy Information Administration. Independent Statistics & Analysis. U.S. Department of Energy.
U.S. EPA, 2016. Hydraulic Fracturing for Oil and Gas: Impacts from the Hydraulic Fracturing Water Cycle on Drinking Water Resources in the United States (Main Report - EPA/600/R-16/236fa). EPA-600-R-16-236Fa. doi:EPA/600/R-15/047a.
Vandecasteele, I., Marí Rivero, I., Sala, S., Baranzelli, C., Barranco, R., Batelaan, O., Lavalle, C., 2015. Impact of shale gas development on water resources: a case study in Northern Poland. Environ. Manag. 55, 1285–1299. https://doi.org/10.1007/s00267-015-0454-8.
Vörösmarty, C., Green, P., Salisbury, J., Lammers, R., 2000. Global Water Resources: Vulnerability from Climate Change and Population Growth. Science 289, 284–288.
Walker, E.L., Anderson, A.M., Read, L.K., Hogue, T.S., 2017. Water use for hydraulic fracturing of oil and gas in the South Platte River Basin, Colorado. JAWRA J. Am. Water Resour. Assoc. 53, 839–853. https://doi.org/10.1111/1752-1688.12539.
Willow, A.J., Zak, R., Vilaplana, D., Sheeley, D., 2014. The contested landscape of unconventional energy development: A report from Ohio's shale gas country. J. Environ. Stud. Sci. 4, 56–64. https://doi.org/10.1007/s13412-013-0159-3.
Wolaver, B.D., Cook, C.E., Sunding, D.L., Hamilton, S.F., Scanlon, B.R., Young, M.H., Xu, X., 2012. Potential economic impacts of environmental flows for central texas freshwater Mussels. Bur. Econ. Geol. Univ. Texas Austin 50, 59. https://doi.org/10.1111/jawr.12171.
Wolaver, B.D., Pierre, J.P., Ikonnikova, S.A., Andrews, J.R., McDaid, G., Ryberg, W.A., Hibbitts, T.J., Duran, C.M., Labay, B.J., LaDuc, T.J., 2018a. An Improved Approach for Forecasting Ecological Impacts from Future Drilling in Unconventional Shale Oil and Gas Plays. Environ. Manag. https://doi.org/10.1007/s00267-018-1042-5.
Wolaver, B.D., Pierre, J.P., Labay, B.J., LaDuc, T.J., Duran, C.M., Ryberg, W.A., Hibbitts, T.J., 2018b. An approach for evaluating changes in land-use from energy sprawl and other anthropogenic activities with implications for biotic resource management. Environ. Earth Sci. 77. https://doi.org/10.1007/s12665-018-7323-8.
WRI, 2014. Global Shale Gas Development, Water Availability and Business Risks. World Resource Institute.
Yang, H., Huang, X., Yang, Q., Tu, J., Li, S., Yang, D., Thompson, J.R., 2015. Water Requirements for Shale Gas Fracking in Fuling, Chongqing, Southwest China. Energy Procedia 76, 106–112.
Yu, M., Weinthal, E., Patiño-Echeverri, D., Deshusses, M.A., Zou, C., Ni, Y., Vengosh, A., 2016. Water Availability for Shale Gas Development in Sichuan Basin, China. Environ. Sci. Technol. 50, 2837–2845. https://doi.org/10.1021/acs.est.5b04669.
Zavala-Torres, R., 2014. Seismic characterization of the Eagle Ford Shale based on rock physics. PhD Thesis. University of Houston.